ISSN 1075-7015, Geology of Ore Deposits, 2006, Vol. 48, No. 3, pp. 151–174. © Pleiades Publishing, Inc., 2006.
Original Russian Text © V.V. Zaikov, I.Yu. Melekestseva, 2006, published in Geologiya Rudnykh Mestorozhdenii, 2006, Vol. 48, No. 3, pp. 179–204.

The Ishkinino Co–Cu Massive Sulfide Deposit Hosted in Ultramafic Rocks of the Main Ural Fault Zone, the Southern Urals

V. V. Zaikov and I. Yu. Melekestseva

Institute of Mineralogy, Uralian Division, Russian Academy of Sciences, Miass, Chelyabinsk oblast, 456317 Russia

Received May 20, 2005

Abstract—The results of study of the Ishkinino Co–Cu massive sulfide deposit hosted in ultramafic rocks of the Main Ural Fault Zone are discussed. The ore field is localized in a fragment of Early Devonian accretionary prism composed of oceanic and island-arc tectonic sheets. The antiform structure of the ore field was formed at the collision stage in the Late Devonian. The primary ore was deposited near the bottom in the environment of the accretionary prism at the island-arc stage of evolution, whereas the superimposed ore mineralization was related to the collision stage. The primary ore is composed of massive, stringer–disseminated, and clastic varieties with two mineral assemblages of sulfides and oxides. The superimposed stringer–disseminated ore mineralization is represented by Co–Ni–Fe arsenides and sulfoarsenides, native gold, Bi and Te minerals, and late sulfides and oxides. Loellingite, safflorite, rammelsbergite, and krutovite were identified in the massive sulfide ore for the first time in the Urals. The geochemical attributes of Co–Ni minerals serve as indicators of superimposed processes. Chromites contained in rocks and ore correspond to Cr-spinel of suprasubduction ultramafic rocks in chemical composition. It is suggested that sulfide ore may be found in the accretionary prisms of the presently active island arcs composed of ultramafic sheets.

DOI: 10.1134/S1075701506030019

INTRODUCTION

The Ishkinino Co–Cu massive sulfide deposit is located in the southern Urals, 20 km west of the town of Gai (Orenburg oblast), in the Main Ural Fault Zone (MUFZ), see Fig. 1. The deposit, hosted in serpentinites, attracts great interest because of the geological setting, untypical of volcanic-hosted massive sulfide orebodies of the Urals. Elevated contents of Ni (as high as 0.5%), Co (up to 0.3%), Cr (up to 0.6%), and Au (as high as 16 g/t) and the occurrence of sulfoarsenides, arsenides, and chromites are the main distinguishing features of this deposit.

The geological exploration of the deposit began in 1928, when the Bashkir Mining Trust developed the oxidized copper ore and cobaltite veinlets were found in prospect holes. Prospecting was carried out in 1929–1933 by the Institute of Applied Mineralogy and the Middle Volga Mining Trust. The efforts of the Ishkinino geological exploration party in 1941–1942 under the supervision of K.D. Subbotin included sinking of exploration workings along with borehole drilling and formed the basis for further investigations.

Subsequently, the geological exploration was supervised by A.P. Sidorenko [1957] and A.G. Poluektov [1965]. The local geology and ore mineralogy were also studied by V.S. Sharfman [1952], G.A. Krutov and E.P. Tsaritsyn [1962], E.S. Kontar [1966], and V.T. Tishchenko [1978]. Some information on the deposit was published by E.S. Buchkovsky, A.S. Varlakov, E.S. Kontar, L.E. Libarova, and V.V. Maslennikov. A review of these studies was given in the monograph by Melekestseva and Zaikov (2003). Our studies of this deposit began in 1998 and included geological mapping on scales of 1 : 2000, 1 : 1000, and 1 : 500. The samples collected were examined under a microscope and analyzed with microprobe, X-ray, and chemical methods.

Corresponding author V.V. Zaikov. E-mail: zaykov@ilmeny.ac.ru

POSITION OF THE DEPOSIT IN THE MAIN URAL FAULT ZONE

The southern flank of the MUFZ, a most important geological suture of Eurasia, is 10–20 km wide and separates metamorphic rocks of the Uraltau from volcanic complexes of the Magnitogorsk island-paleoarc system (Fig. 1). In tectonic schemes, this segment is designated as the Cis-Sakmara–Voznesenka lithotectonic zone. The Ishkinino deposit is located in the Gai ore district, one of the most productive in terms of Cu and Zn reserves throughout the West Magnitogorsk island-paleoarc system. The Ivanovka and Dergamysh Co–Cu massive sulfide deposits are also associated with ultramafics and are similar in this respect to the Ishkinino deposit; they occur to the northwest of the latter in the Baimak–Buribai district. The evolution of geological complexes of the MUFZ is subdivided into several stages (Puchkov, 2000): rifting (Middle Ordovician–

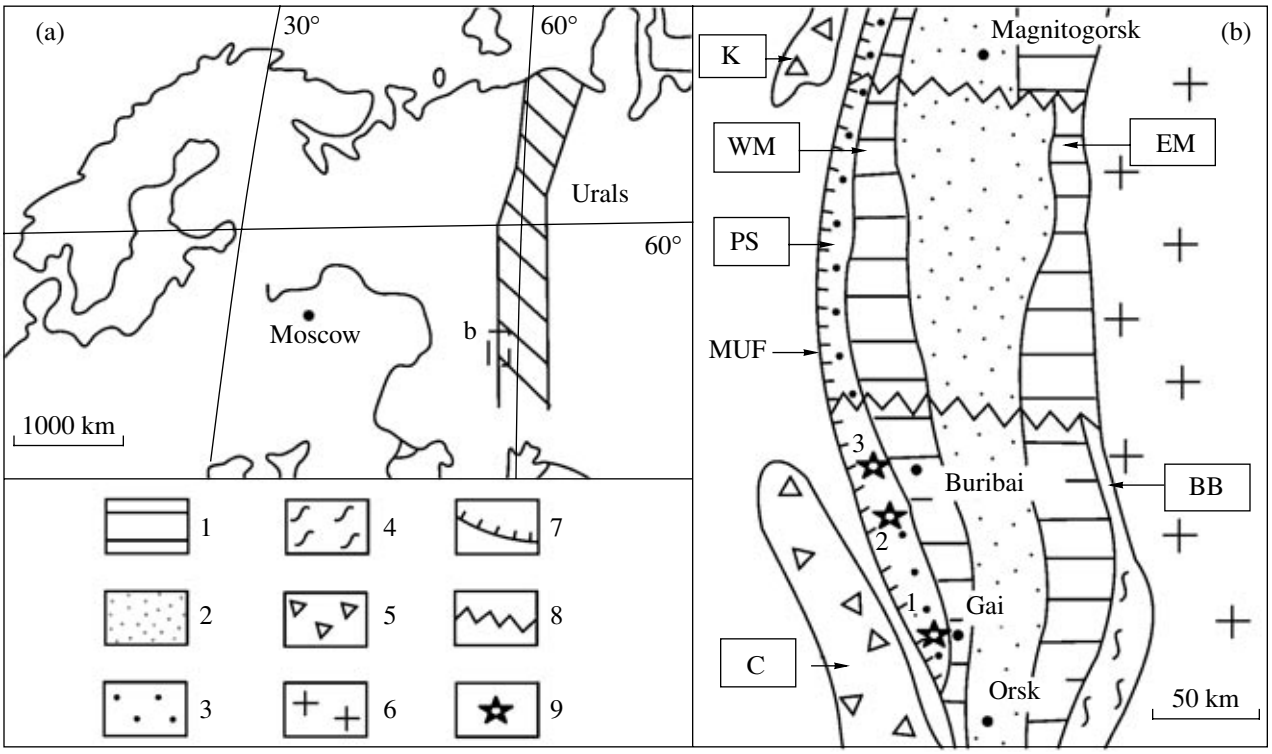

Fig. 1. (a) Index map and (b) geological setting of Co–Cu massive sulfide deposits in the southern Urals. (1) Island paleoarcs (WM—West Magnitogorsk, EM—East Magnitogorsk); (2) Magnitorgorsk interarc basin; (3, 4) ophiolitic zones: (3) Cis-Sakmara (PS is a fragment of Paleozoic subduction zone), (4) Dombarovka (BB is a backarc basin behind the East Magnitogorsk island arc); (5) marginal allochthons (S—Sakmara, K—Kraka); (6) East Ural Rise; (7) Main Ural Fault (MUF); (8) hidden transverse faults that bound the segments of the Paleozoic island-arc system; (9) Co–Cu massive sulfide deposits.

Silurian), when the oceanic crust was formed; subduction (Early and Middle Devonian), responsible for the development of island-arc volcanic complexes and olistostromes; and collision (Late Devonian–Early Permian), which gave rise to the formation of melange zones and strike-slip faulting. The lying wall of the fault zone in the study territory consists of volcanosedimentary sequences that underwent low-temperature–high-pressure metamorphism. The section comprises intercalating metabasic rocks, microquartzite, metagraywacke, and serpentinite sheets. These rocks host sulfide lenses (the Yuluk and Gumerovo deposits) similar to massive sulfide deposits of the MUFZ in ore composition.

The axial zone of the MUFZ is filled with serpentinite melange, with blocks of Ordovician–Silurian ophiolites and Devonian–Carboniferous volcanosedimentary rocks incorporated into the melange. The largest blocks are 2–4 km across; they are either enveloped or parted by serpentinites. The ultramafic sheets are deformed into syn- and antiforms together with sheets of volcanic and sedimentary rocks. Zones of talc–carbonate metasomatism replace ultramafic rocks and partly massive sulfide lodes. Blocks of Devonian rocks, the Upper Devonian–Lower Carboniferous, the Zilair Flysch included, are predominant in the eastern hanging wall of the suture zone.

GEOLOGY OF THE DEPOSIT

The deposit is related to an antiform that consists of three tectonic sheets (Figs. 2, 3) composed of serpentinites, basalts, and cherts. The ore mineralization is localized at the roof of serpentinite sheet and is accompanied by talc–carbonate metasomatic rocks replacing serpentinite. The ore field is bounded in the west and east by meridional, steeply dipping strike-slip faults.

The lower sheet (Sakmara Formation, Ssk) is penetrated by boreholes in the antiform core at a depth of 300–700 m. At the surface, this sheet is exposed in the northern ore field as tectonic blocks divided by serpentinite protrusions. The sheet consists of three units composed of basalt, plicated platy quartzite, carbonaceous siltstone and sandstone with remains of Silurian graptolites, mixtite with a cherty matrix, and fragments and blocks of quartzite and less frequent basalt and limestone (Fig. 3). Volcanics of the Sakmara Formation are close in chemical composition to E-MORB and backarc basin basalts (Table 1). In REE content (Jonas, 2003), these rocks are comparable with N-MORB.

The middle sheet is composed of serpentinites developing after harzburgite and dunite (Fig. 3). The former are located in the central part of the antiform, while the latter occur as separate blocks at antiform limbs. Serpentinites are crossed by near-meridional melange zones 5–30 m wide that commonly divide

Table 1. Chemical composition of basaltic rocks at the Ishkinino deposit, wt %

No.	Sample	SiO_2	TiO_2	Al_2O_3	Fe_2O_3	MnO	MgO	CaO	Na_2O	K_2O	H_2O	P_2O_5	LOI	Total
						Sakmara Complex								
1	679-7	45.15	2.08	13.38	12.20	0.22	6.11	7.77	4.62	0.25	0.00	0.44	6.59	99.81
2	709-11	55.06	0.85	16.10	8.64	0.15	3.20	5.80	3.44	1.38	0.10	0.36	3.92	99.96
3	679-3	53.38	0.78	13.92	9.12	0.16	7.11	7.24	2.79	0.19	0.00	0.14	4.75	99.78
4	679-5	51.42	0.64	15.40	8.73	0.17	5.71	8.60	5.21	0.73	0.00	0.15	3.04	99.81
5	679-6	51.21	1.02	13.44	12.29	0.25	4.48	7.73	2.97	0.18	0.00	0.19	6.64	100.41
						Baimak–Buribai Complex								
						The western limb of the antiform								
6	35-2	57.35	0.55	13.41	9.09	0.23	5.04	6.28	6.58	0.33	0.00	0.06	1.48	100.40
7	35-3	54.59	0.46	15.88	9.91	0.23	4.21	3.93	8.48	0.16	0.00	0.06	3.14	101.06
8	40-1	55.69	0.65	16.20	8.95	0.13	3.40	4.33	7.68	0.22	0.00	0.08	2.96	100.30
9	40-3	61.05	0.62	13.34	9.08	0.14	4.22	2.55	6.53	0.27	0.00	0.08	2.64	100.53
10	42	56.56	0.54	15.23	8.17	0.11	5.70	5.04	3.54	0.09	0.16	0.10	4.52	99.76
11	42-1	52.12	0.48	14.96	10.05	0.17	8.50	5.28	3.52	0.14	0.34	0.10	4.10	99.76
12	42-2	51.30	0.48	16.64	7.15	0.11	4.10	14.49	0.20	0.09	0.10	0.11	5.24	99.91
13	617-6	55.10	0.51	16.26	7.00	0.08	6.58	7.25	4.05	0.90	0.20	0.10	1.70	99.98
14	648-2	53.52	0.32	16.43	7.00	0.10	7.78	3.92	5.65	0.22	0.38	0.07	3.74	99.37
15	648-3	53.83	0.39	15.64	6.90	0.11	8.74	3.28	6.50	0.29	0.38	0.08	3.06	99.38
16	680-6	57.31	0.49	14.66	6.30	0.10	6.18	6.79	5.12	0.40	0.09	0.07	1.82	99.43
17	680-5	54.50	0.56	14.87	7.40	0.12	7.24	6.94	3.48	1.12	0.09	0.07	3.12	99.64
						The eastern limb of the antiform								
18	S-7A-99	52.23	0.6	16.39	9.31	0.19	7.34	6.97	3.55	0.73	0.00	0.05	2.77	100.13
19	S-7C-99	56.51	0.65	15.53	7.79	0.08	4.80	6.49	4.44	0.37	0.00	0.08	2.62	99.36
20	S-8C-99	62.22	0.46	13.4	6.98	0.11	5.39	4.15	4.25	0.09	0.00	0.06	2.16	99.26
21	S-8D1-99	58.98	0.44	11.32	10.07	0.19	7.53	6.81	3.19	0.08	0.00	0.04	1.21	99.87
22	S-8E-99	61.28	0.66	14.48	5.90	0.09	4.23	6.28	3.81	0.23	0.00	0.06	3.07	100.10
23	S-8G-99	59.51	0.68	13.71	7.29	0.11	5.50	7.92	3.56	0.05	0.00	0.06	1.74	100.14
24	S-9A-99	51.93	0.54	13.06	9.13	0.19	10.67	6.90	2.28	0.04	0.00	0.05	5.03	99.81
25	S-9B-99	52.04	0.58	14.05	8.66	0.15	10.50	7.01	2.29	0.39	0.00	0.03	3.97	99.68
26	S-9C-99	53.53	0.54	13.20	8.74	0.18	10.21	6.10	2.40	0.05	0.00	0.04	4.63	99.62
27	S-5B-99	49.43	0.72	14.73	9.31	0.14	3.76	16.05	1.15	0.07	0.00	0.12	4.33	99.80
28	S-6-99	53.45	0.77	15.58	11.18	0.21	4.21	6.25	3.02	0.66	0.00	0.10	4.59	100.02
29	S-12A-99	60.02	0.80	13.75	10.76	0.17	3.46	4.41	2.71	0.19	0.00	0.12	3.72	100.11
30	S-12B-99	56.19	0.84	14.48	10.05	0.18	3.99	7.73	2.13	0.17	0.00	0.12	3.98	99.85
31	S-12D-99	51.85	0.58	14.95	9.08	0.16	5.62	9.81	3.39	0.72	0.00	0.07	3.77	100.01

Note: (1, 2) Dikes, (3–5) lavas, (27–31) lavas. Samples were taken from collections of R.R. Shavaleev and V.V. Zaikov (6–14) and V.A. Simonov (15–31). Samples 1–17 were analyzed at the chemical laboratory of the Institute of Mineralogy, Uralian Division, Russian Academy of Sciences, analyst T.V. Semenova. Samples 18–31 were analyzed at the chemical laboratory of the United Institute of Geology, Geophysics, and Mineralogy, Siberian Division, Russian Academy of Sciences, Novosibirsk.

apodunitic and apoharzburgitic varieties and contain boudins of all serpentinite varieties up to a few meters in size. Ribbon banding and asbestos veinlets occur at contacts between apodunitic and apoharzburgitic serpentinites. Serpentinites are replaced by carbonate, talc, and chlorite.

Apodunitic serpentinite is a dark green massive rock composed of β-lizardite (occasionally α-lizardite) with a polygonal–grained loop structure with loops up to 1.5 mm in size (Varlakov, 1978; Dunaev and Churin, 2003). Apoharzburgitic serpentinite is a green rock containing 30–35% large bastite crystals. Serpophite, anti-

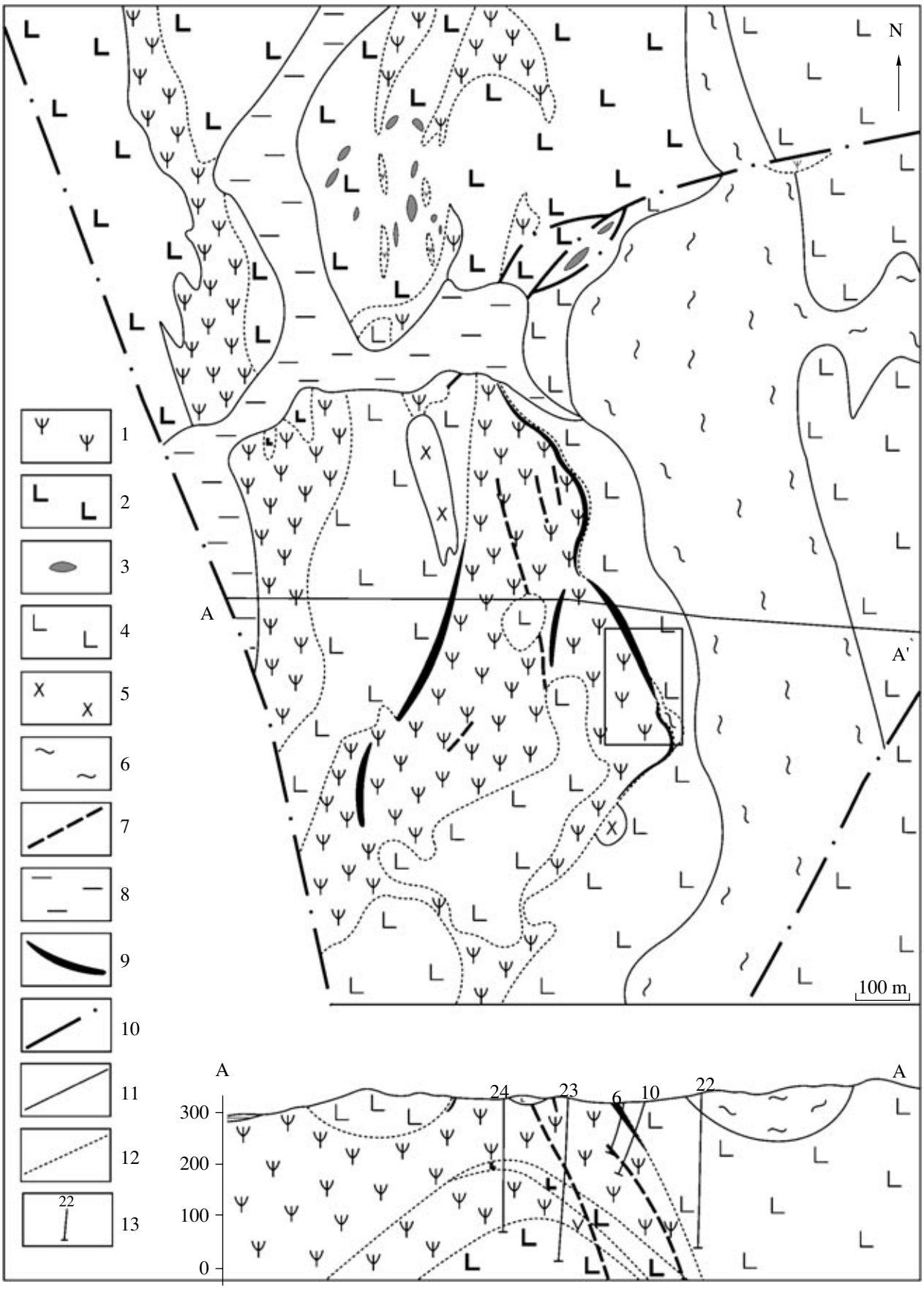
N
A
A'
100 m
1
2
3
4
5
6
7
8
9
10
11
12
13
22
A
A
300
200
100
0
24
23
6
10
22

Table 2. Chemical composition of serpentinites at the Ishkinino deposit, wt %

No.	Sample	SiO_2	TiO_2	Al_2O_3	FeO*	MnO	MgO	CaO	Na_2O	K_2O	H_2O	P_2O_5	LOI	Total
1	D-879	39.77	0.03	1.67	12.04	0.12	33.06	0.10	0.30	0.10	–	0.03	12.49	99.73
2	D-880	40.53	0.03	1.78	9.53	0.16	34.56	0.07	0.30	0.09	–	0.03	12.81	99.90
3	D-881	39.90	0.03	1.79	10.05	0.07	34.81	0.06	0.32	0.09	–	0.03	12.64	99.81
4	D-882	40.28	0.03	1.58	9.87	0.06	34.65	0.05	0.57	0.09	–	0.03	12.71	99.94
5	D-883	40.04	0.03	1.92	11.15	0.10	33.67	0.07	0.58	0.10	–	0.03	12.50	100.20
6	D-884	39.20	0.03	1.65	13.41	0.10	33.13	0.09	0.30	0.10	–	0.03	12.08	100.13
7	D-888	41.26	0.03	1.79	8.52	0.08	34.61	0.07	0.57	0.11	–	0.03	12.89	99.97
8	D-889	40.56	0.03	2.19	8.01	0.07	35.21	0.06	0.30	0.09	–	0.03	12.83	99.40
9	D-895	40.30	0.03	2.09	8.73	0.10	34.71	0.05	0.30	0.09	–	0.03	13.28	99.73
10	D-885	40.25	0.03	1.69	9.08	0.08	35.35	0.04	0.30	0.10	–	0.03	12.91	99.88
11	D-886	41.05	0.03	1.96	7.84	0.05	35.36	0.06	0.30	0.10	–	0.03	13.22	100.02
12	D-887	40.98	0.03	1.75	8.43	0.08	35.33	0.06	0.30	0.10	–	0.03	12.93	100.04
13	M-1	39.48	<0.05	0.51	8.13	0.13	36.83	0.61	0.09	<0.02	0.88	<0.05	12.62	99.28
14	M-3	36.90	<0.05	0.63	13.20	0.09	35.37	0.48	0.11	<0.02	1.06	<0.05	12.22	100.06
15	M-4	37.14	0.17	5.28	6.74	0.18	35.10	0.92	0.10	<0.02	1.18	<0.05	13.26	100.07
16	M-5	39.14	<0.05	0.22	8.47	0.15	37.47	0.45	0.10	<0.02	0.62	<0.05	12.40	99.96
17	M-6	36.72	<0.05	0.44	13.40	0.06	35.42	0.45	0.08	<0.02	1.06	<0.05	11.94	99.57
18	M-17	37.80	0.05	0.42	10.90	0.05	36.95	0.34	0.07	n.d.	0.82	<0.05	12.20	99.60
19	M-8	36.92	<0.05	0.61	9.60	0.08	36.30	2.14	0.10	<0.02	0.66	<0.05	13.14	99.55
20	618-5	40.99	<0.05	0.21	6.92	0.15	37.28	0.46	0.08	<0.02	0.92	n.d.	12.94	99.95
21	618-25	39.30	<0.05	0.30	8.08	0.05	38.91	0.33	0.14	<0.02	0.58	<0.05	12.30	99.99
22	647-12	39.07	n.d.	1.96	9.85	0.10	36.12	0.40	0.04	0.03	0.49	0.03	11.89	99.98

Note: (1–9, 13, 14, 16–19, 22) Serpentinite after dunite; (10–12, 15, 21) serpentinite after harzburgite. Samples were taken from collections of A.Yu. Dunaev (1–12), I.Yu. Melekestseva (13–19), and V.V. Zaikov (20–23). Samples 1–12 were analyzed at the chemical laboratory of the United Institute of Geology, Geophysics, and Mineralogy, Siberian Division, Russian Academy of Sciences, Novosibirsk. Samples 13–22 were analyzed at the chemical laboratory of the Institute of Mineralogy, Uralian Division, Russian Academy of Sciences, analysts T.V. Semenova and Yu.F. Mel'nova. A dash denotes not analyzed and n.d. denotes not detected. FeO* is total iron.

gorite, ophite, chrysotile, talc, brucite, chlorite, carbonates, magnetite, and sulfides occur in serpentinites.

Serpentinites developing after dunite and harzburgite are close in chemical composition (Table 2). The Cr content in serpentinites ranges from 0.05 to 0.77 wt % (Varlakov, 1978). Apoharzburgitic serpentinite is slightly enriched in Ni relative to the apodunitic variety (0.19 against 0.15 wt %). The Co content in serpentinites varies from 0.005 to 0.019 wt %. The average Ni content in serpentinites partially replaced by talc and carbonates reaches 0.42 wt %.

The ore-bearing conglomerate-like serpentinites at the roof of the ultramafic sheet occur as interlayers 1−12 m thick; rounded fragments 1–5 cm (occasionally up to 40 cm) in diameter are composed of serpentinized harzburgite and dunite and pyroxenite. The psammitic–psephitic cement consists of serpentinite, fragments of pyroxene crystals, and sulfide clasts. The psammitic and psephitic particles are incorporated into a fine flaky mass consisting of chrysolite, antigorite, serpophite, talc, and chlorite. Both fragments and cement are replaced by carbonates, talc, chlorite, and sulfides. The roof of the serpentinite sheet is complicated by a

Fig. 2. Geological map of the Ishkinino Co–Cu massive sulfide deposit. Compiled by V.V. Zaikov and I.Yu. Melekestseva using the data of K.D. Subbotin, A.P. Sidorenko, and A.G. Poluektov. (1) Ordovician–Early Silurian (?) serpentinites after dunite and harzburgite, including melange zones and zones of talc–carbonate metasomatic rocks; (2, 3) Silurian–Devonian Sakmara Complex: (2) basalt, quartzite, dolerite sills and dikes, (3) limestone lenses; (4, 5) Early Devonian Baimak–Buribai Complex: (4) basalt, basaltic andesite, volcanomictic olistostrome; (5) diorite and gabbrodiorite, basaltic dikes; (6) Middle Devonian Ishkinino Complex: silicite, volcanomictic cherty olistostrome; (7) Early Carboniferous (?) Khudolazovo Complex: gabbropegmatite dikes; (8) Quaternary alluvial sediments and talus; (9) ore-bearing zones with Co–Cu massive sulfide ore (not scaled); (10) faults; (11) boundaries of stratigraphic subdivisions and intrusive bodies; (12) boundaries of serpentinite sheets; (13) exploration boreholes. The rectangle is the area shown in Fig. 4.

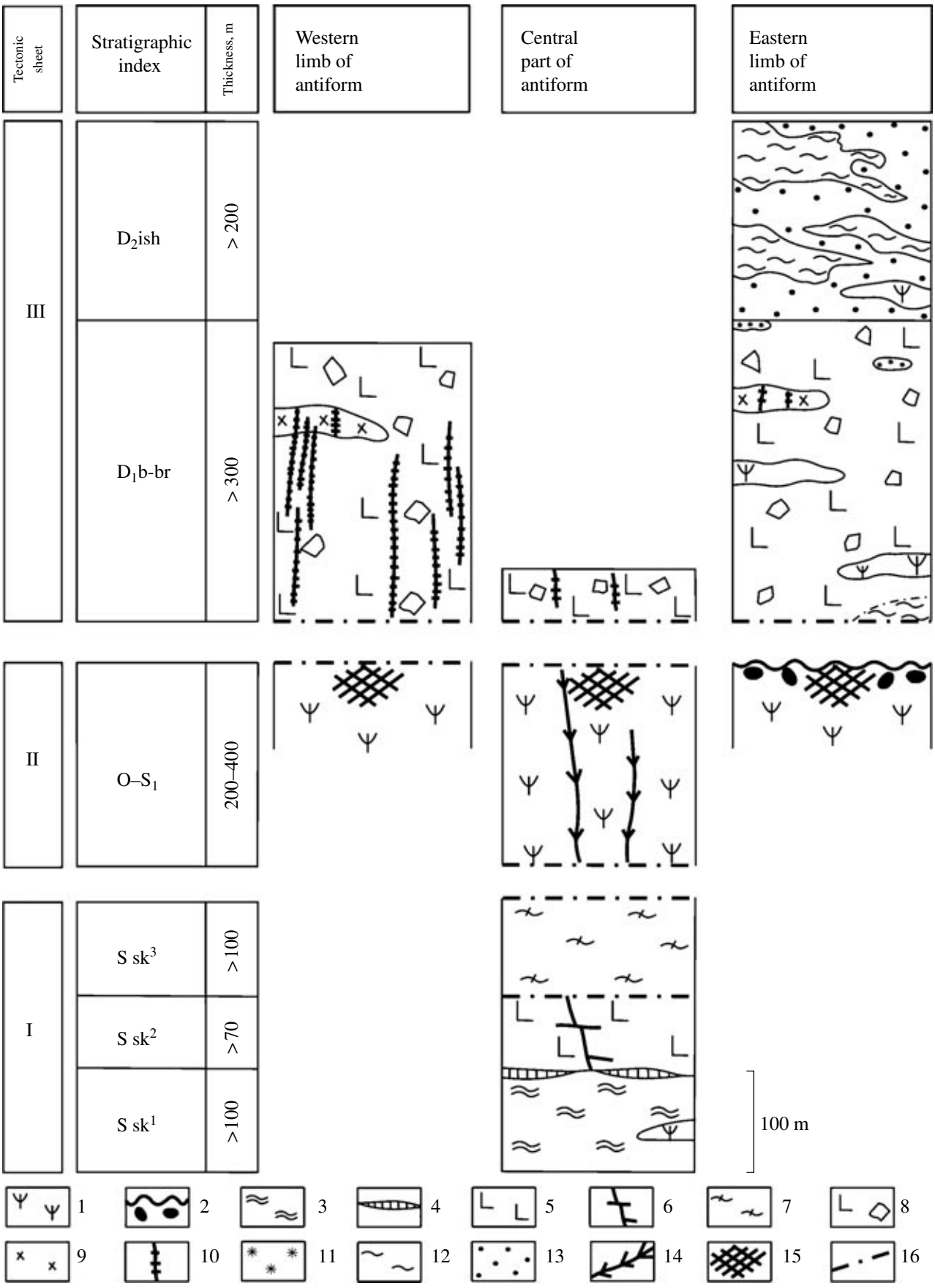
Tectonic sheet
Stratigraphic index
Thickness, m
Western limb of antiform
Central part of antiform
Eastern limb of antiform
III
D2ish
> 200
D1b-br
> 300
II
O–S1
200–400
I
S sk3
> 100
S sk2
> 70
S sk1
> 100
100 m
1
2
3
4
5
6
7
8
9
10
11
12
13
14
15
16

melange zone, which, in the opinion of previous investigators, indicates the tectonic nature of the conglomerate-like serpentinite. However, olistostromes with serpentinite breccias and sandstones were found in the MUFZ (Seravkin et al., 2003), and the aforementioned rocks may also be of sedimentary origin.

The upper sheet is composed of volcanic and sedimentary sequences (Fig. 3). The Lower Devonian Baimak–Buribai Sequence (D_1 b-br) consists of disintegrated lavas and edaphogenic breccia of olistostrome nature with large olistoliths of gabbro and diorite as long as 300 m and a few tens of meters thick that are cut by basaltic dikes. Blocks of dacite and rhyolite are less abundant. The chemical composition of volcanic rocks (Table 1) fits island-arc volcanics close to boninites (Simonov et al., 2000).

The sedimentary Middle Devonian Ishkinino Sequence (D_2 ish) corresponds to the level of the Yarlykapovo Horizon and the Turat Formation, which overlie the Irendyk Complex and replace it in the lateral direction (*Stratigraphy*..., 1993). This sequence consists of cherty and cherty–clayey sedimentary rocks with predominant phtanites that contain remains of the Emsian and early Eifelian conodonts *Polygnatus ex. gr. costatus* and *P. aff. pseudofoliatus* (*Stratigraphy*..., 1993); interlayers of red jasper, mudstone, sandstone, and volcanomictic rocks are noted, as well as limestone lenses with Early Devonian–early Eifelian benthic fauna. The chert beds are laterally replaced by volcanomictic–cherty olistostrome with phtanitic olistoliths up to 50 m long deformed into disharmonic folds. The transition from volcanomictic to cherty olistostrome is gradual; the transitional member, a few tens of meters thick, is characterized by the appearance of cherty agglomerate fragments and olistoliths associated with basaltic lava breccia. The amount of such fragments gradually increases, and sedimentary material with sporadic volcanomictic lenses becomes prevalent up the section. The transitional member contains ultramafic bodies a few tens of meters long, which are accompanied by serpentinite breccia. Blocks of chromite-bearing ophicalcite breccia 2–3 m in size appear in the volcanomictic and cherty olistostromes.

Zones of tectonic breccia 2–5 m thick are observed at the contact between the serpentinite and olistostrome sheets. Chromite and serpentinite fragments occur in sandstone from the volcanomictic sequence. The basaltic dikes that cut through the volcanic Baimak–Buribai Formation do not penetrate into the serpentinite sheet. This indicates that the olistostrome sheet was formed on the eroded surface of serpentinite but afterwards detached along the lower contact.

CHARACTERISTICS OF ORE ZONES

During geological exploration in the 1940–1960s, the ore was crossed by boreholes, adits, and deep prospect holes with drifts and insets. Subbotin distinguished the near-meridional Western, Central, and Eastern ore zones (Fig. 2). The most detailed exploration with underground workings was carried out in the central part of the Eastern Zone.

The Eastern ore zone embraces the contact between serpentinite and basaltic sheets (Fig. 4). Mineralized conglomerate-like serpentinite that hosts massive sulfide lenses and talc–carbonate metasomatic rocks with stringer–disseminated and brecciated sulfide mineralization occur in this zone, which extends for ~800 m with a width (in plan view) of 80–100 m. The central part of the zone 200 m long was crossed by 16 underground workings to a depth of 30 m; orebodies occur in the depth interval from 25 to 90 m. Conglomerate-like serpentinite hosts 15 lenticular bodies of massive sulfide ore that grades into stringer–disseminated mineralization. The orebody thickness varies from 0.3 to 2.0 m; their extent along the strike and down the dip ranges from 0.5–2.0 to 30–65 m and from 20 to 30 m, respectively. The orebodies steeply dip at angles of 65°–80° parallel to the contact between sheets. Twenty-six lenticular bodies of massive and disseminated ores were delineated in talc–carbonate metasomatic rocks. The ore lenses are 0.3–5.5 m thick and extend for 15–163 m along the strike and 13–60 m down the dip. Serpentinite breccia and ore with carbonate cement are widespread in zones of talc–carbonate rocks. The breccia bodies are 2–4 m thick and as long as 200 m; they gently dip eastward.

The Central ore zone, 150 m long and a few meters thick, is related to the melange zone that divides blocks of serpentinites after dunite and harzburgite. The ore mineralization was traced to a depth of 24 m.

The Western ore zone is localized at the western limb of the antiform and confined to a body of talc–carbonate metasomatic rocks of complex morphology. Northern and southern areas are recognized; both are

Fig. 3. Lithologic columns of tectonic sheets at the Ishkinino deposit. Compiled by V.V. Zaikov and I.Yu. Melekestseva using the data of K.D. Subbotin, A.P. Sidorenko, A.G. Poluektov, and V.G. Tishchenko. (1, 2) Ultramafic complex ($O–S_1$?): (1) (?) serpentinites after dunite and harzburgite, including melange zones, zones of serpentinites replaced with carbonate, talc, and chlorite, and zones of talc–carbonate metasomatic rocks; (2) erosion surface of serpentinite sheet with ore-bearing conglomerate-like serpentinite and overlapping clastic ore; (3–7) Sakmara Complex ($S–D_1$sk): (3) platy quartzite with members of mixtites and basaltic flows, (4) limestone interlayers, (5) basalts with mixtite members and quartzite interlayers, (6) dolerite and microdiorite sills and dikes ($v\mu S_1$), (7) quartzite and carbonaceous siltstone with graptolite remains; (8–11) Baimak–Buribai Complex (D_1b-br): (8) basalt, basaltic andesite, volcanomictic breccia, (9) gabbro and diorite olistoliths (δ, $v\mu D_1$), (10) basaltic dike ($v\mu D_1$), (11) olistolith of serpentinite–carbonate breccia; (12, 13) Ishkinino Complex (D_2ish): (12) phtanite, jasper, mudstone, sandstone, (13) sandy matrix of olistostrome; (14–16) Khudolazovo Complex (vC_1?): (14) gabbropegmatite and pyroxenite dikes, (15) Co–Cu massive sulfide ore, (16) faults.

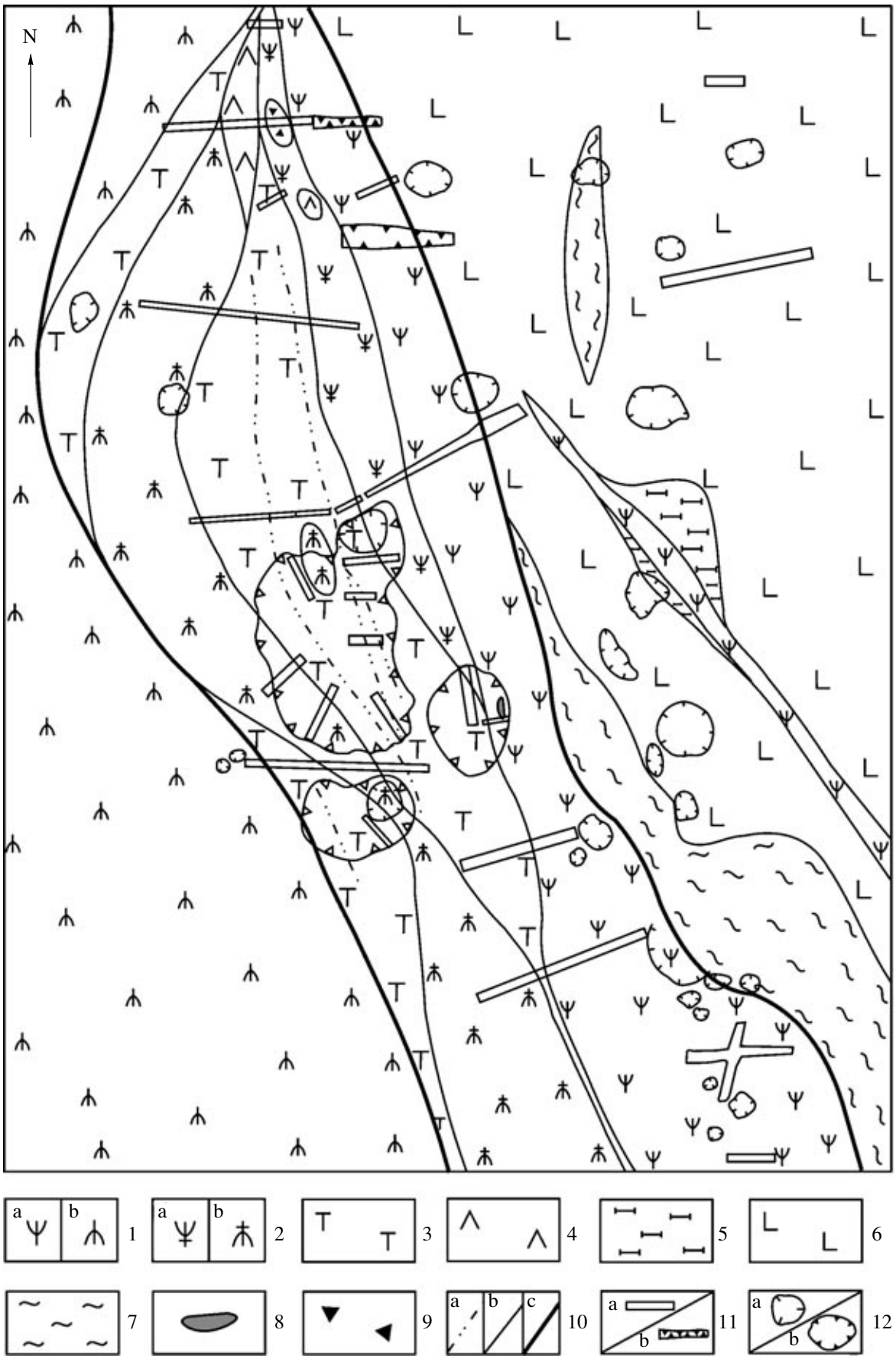
N
a b 1
a b 2
3
4
5
6
7
8
9
a b c 10
a b 11
a b 12

540 m long and 50–60 m wide. Fragments of sulfide ore were found in prospect holes 12 and 14 at a depth of 20–22 m. In the southern area, two small ancient pits 7 and 8 stripped altered serpentinite and limonitized metasomatic rocks with abundant secondary copper mineralization. R.R. Shavaleev and A.M. Yuminov revealed sporadic gold grains in serpentinite partly replaced by talc and talc–carbonate metasomatic rocks.

The composition of ore lodes. Subbotin subdivided the ores into massive (pyrite–pyrrhotite and cobaltite–chalcopyrite–pyrrhotite) and disseminated (arsenopyrite–cobaltite) varieties. Pyrrhotite, pyrite, chalcopyrite, magnetite, chromite, nickeline, cobaltite, arsenopyrite, cubanite, sphalerite, marcasite, and pentlandite have been identified as ore minerals. Serpentine, chlorite, carbonate, and quartz are gangue minerals.

The following chemical composition of ores was determined in the course of the geological exploration (wt %): (1) pyrite–pyrrhotite ore: up to 0.1 Co (0.03 on average), up to 2 Cu (0.6 on average), 0.2–0.3 Ni, and 28–30 S; (2) cobaltite–chalcopyrite–pyrrhotite ore: up to 1–10 Co (0.30 on average), 0.5–15 Cu (6.4 on average), 0.1–0.4 Ni, 0.4 Zn, 1 ppm Pt, 4–6 ppm Ag, and 1.4 ppm Au; (3) disseminated ore: 0.01–0.12 Co (0.06 on average) and 0.5–2.0 Cu (0.7 on average).

The ore is classified as copper (>0.5–0.7% Cu; <0.8–1.0% Zn) and disseminated economic (technological) sort (as high as 35% S). The approximate qualitative characteristic of the ore ranges from low-grade (0.5% Cu) to medium-grade (1.04% Cu) and high-grade (up to 15–17% Cu).

ORE TYPES

Samples of massive, stringer–disseminated, and clastic ores from dumps of deep prospect holes in the Eastern ore zone were collected for the study (Fig. 4).

The massive ore is represented by three mineral types: pyrite–pyrrhotite, chalcopyrite–pyrite–pyrrhotite, and sulfoarsenide–sulfide.

(1) The pyrite–pyrrhotite ore is massive, brecciated, or spotty and consists of pyrrhotite (70–80%), pyrite (15–20%), chalcopyrite (1–5%), magnetite, and chromite (5%). The brecciated structure is emphasized by rounded and lenticular fragments of pyrrhotite composition parted by pyrite veins; the spotty structure is caused by magnetite spots in pyrrhotite.

(2) The chalcopyrite– pyrite–pyrrhotite ore is massive and banded. The widespread brecciated ore consists of older pyrite–pyrrhotite aggregates cemented by younger chalcopyrite. Pyrrhotite (20–60%), pyrite (10–20%), chalcopyrite (10–70%), magnetite, and chromite (5%) are visible to the naked eye. Chalcopyrite is predominant (up to 70%) in many samples.

(3) The cobaltine–arsenopyrite–chalcopyrite–pyrite–pyrrhotite (sulfoarsenide–sulfide) type is characterized by veined, crudely banded, massive, and brecciated structures. The ore consists of pyrrhotite (40–50%), pyrite, chalcopyrite (10–20%), cobaltite and arsenopyrite (10–30%), and magnetite and chromite (5% each of both minerals). Cobaltite and arsenopyrite occur as veins up to 10 cm thick and as disseminated crystals from 1–2 to 3–5 mm (intergrowths) in size within sulfides and carbonate veins.

The stringer–disseminated ore is subdivided into pyrite–pentlandite–pyrrhotite, chalcopyrite–pyrite–pyrrhotite, pyrite–chalcopyrite–pyrrhotite, and chalcopyrite types.

The disseminated pyrite–pentlandite–pyrrhotite ore is hosted in serpentinite. The content of ore minerals is about 10%. The chalcopyrite-bearing ore occurs in the metasomatic rocks that replace serpentinite and in breccia consisting of serpentinite fragments and carbonate cement. Brecciated–disseminated, pocket–disseminated, stringer, and banded disseminated structures are typical. Breccia is composed of apodunitic serpentinite fragments of various shapes and from a few millimeters to 5–7 cm in size. The ore fragments consist of pyrrhotite, chalcopyrite, and pyrite from a few millimeters to 5 cm in size.

The clastic ore is represented by serpentinite–sulfide gravelstone (Fig. 5a) and sandstones with a basal and occasionally porous silty cement that consists of lizardite chloritized to various degrees and of ore dust (Melekestseva and Zaikov, 2003). Sandstones are fine-, medium-, and coarse-grained. The lithic fragments comprise (1) lizardite with antigorite sheets partly or completely replaced with chlorite; (2) fragments and relics of pyroxene and olivine partly replaced with lizardite, antigorite, chrysotile, and chlorite; (3) serpentine completely replaced with chlorite; and (4) calcite. Chromite occurs both in serpentinite fragments and as isolated clasts (Fig. 5b). The ore fragments are composed of pyrite, pyrrhotite, chalcopyrite, and magnetite with widespread concentrically zoned and colloform structures of fragments.

The collected hand specimens were analyzed with INAA (Table 3). PGE were determined at the Laboratory of Activation in Canada and at the Institute of

Fig. 4. Geological map of the Eastern ore-bearing zone at the Ishkinino Co–Cu massive sulfide deposit. Compiled by V.V. Zaikov, I.Yu. Melekestseva, and A.M. Yuminov using the data of K.D. Subbotin, A.P. Sidorenko, and A.G. Poluektov. (1) Serpentinites: (a) after dunite, (b) after harzburgite; (2) carbonated serpentinite: (a) after dunite, (b) after harzburgite; (3) talc–carbonate metasomatic rocks after serpentinite; (4) listvenite?; (5) pyroxenite; (6) basaltic volcanomictic breccia with olistoliths of silicite, jasper, and carbonate breccia; (7) phtanite with sandstone interlayers; (8) lens of brown apodunitic serpentinite with abundant impregnation of Cr-spinel; (9) breccia with carbonate cement and fragments of serpentinite, pyrite–pyrrhotite, and chalcopyrite–pyrite–pyrrhotite ores; (10) linear structures: (a) series of carbonate veins in metasomatic rocks, (b) boundaries of geological bodies, (c) contour of ore zone; (11) trenches driven in (a) the 1940–1960s and (b) 2001; (12a) prospect holes sunk in the 1940–1960s, (12b) ancient open pits.

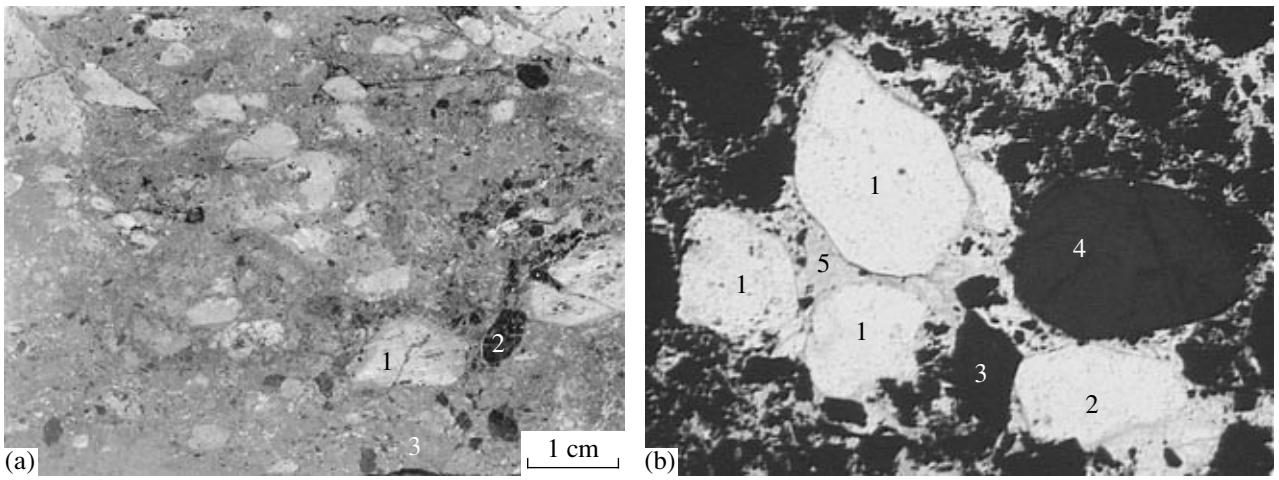

Fig. 5. Clastic ore at the Ishkinino deposit. (a) Serpentinite–sulfide medium-clastic gravelstone: (1) sulfide fragments, (2) lithic fragments, (3) basal ore and occasionally porous lithic cement. Polished specimen 610-12. (b) Serpentinite–sulfide fine-grained sandstone: (1) lizardite completely replaced with chlorite, (2) lizardite replaced with chlorite along the fragment margins, (3) sulfide clasts, (4) chromite, (5) cement composed of chloritized fine flaky lizardite with ore dust, sample 610-E. Photomicrograph of thin section (plane light) 0.79 mm in natural width.

Geology and Geochemistry in Yekaterinburg, Russia, but the contents turned out to be below the detection limit. The Au, Ag, As, Co, and Sb contents increase from the pyrite–pyrrhotite ore to the sulfoarsenide–sulfide ore, where they reach 16.9 ppm Au, 6.1 ppm Ag, 26.1% As, 0.3% Co, and 160 ppm Sb. The highest Cu content (up to 21%) was detected in the chalcopyrite–pyrite–pyrrhotite type of ore along with elevated contents of Co, Cr, and Ni (0.2, 0.6, and 0.3%, respectively).

Table 3. Chemical composition of ore at the Ishkinino deposit (INAA results)

Sample	Fe	S	Cu	Co	Cr	Ni	As	Mn	Au	Ag	Zn	Pb	Sb	Sc	Se	Bi	V
1	54.9	24.2	0.64	0.01	0.33	0.27	0.04	0.14	0.2	3.4	6	n.d.	n.d.	0.6	14	n.d.	2
2	62.3	28.3	0.45	0.01	0.45	0.22	0.06	0.05	1.0	1.4	21	7	0.4	0.7	13	11	2
3	57.2	28.4	1.38	0.01	0.43	0.35	0.07	0.05	0.8	3.4	30	11	0.2	0.9	18	10	2
4	50.7	26.8	10.0	0.05	0.45	0.24	0.22	0.05	0.8	5.2	448	7	n.d.	1	90	53	3
5	64.4	27.6	0.36	0.01	0.41	0.22	0.21	0.06	0.3	0.8	2	n.d.	″	8.1	19	n.d.	2
6	48.3	27.8	1.78	0.03	0.42	0.22	0.18	0.03	2.7	2.8	67	7	0.3	0.6	16	5	3
7	55.5	30.5	0.60	0.02	0.34	0.13	0.67	0.08	1.7	1.2	8	15	n.d.	24.9	43	10	4
8	45.4	29.3	3.43	0.05	0.08	0.13	4.75	0.06	3.4	3.7	164	20	32.7	2.4	23	10	2
9	54.5	31.0	0.71	0.03	0.40	0.26	0.34	0.07	1.4	2.3	3	n.d.	0.5	0.2	30	n.d.	2
10	56.7	27.3	0.65	0.01	0.33	0.15	0.08	0.06	1.7	2.2	35	12	0.8	1.2	9	5	3
11	55.0	28.1	5.11	0.14	0.44	0.45	3.64	0.04	6.6	5.0	156	8	30.5	9.2	14	19	3
12	50.0	28.4	6.40	0.07	0.49	0.25	0.12	0.04	1.0	9.0	243	9	1.5	6.9	51	20	7
13	49.5	26.5	6.96	0.07	0.34	0.26	2.69	0.08	3.2	3.8	317	9	16.5	1.6	19	15	2
14	51.9	23.1	0.29	0.01	0.19	0.21	0.02	0.17	0.1	3.3	2	n.d.	0.3	0.6	15	n.d.	2
15	43.2	26.6	10.0	0.16	0.32	0.25	0.12	0.03	0.5	11.6	750	10	1.1	1.1	135	″	6
16	39.2	20.0	9.29	0.18	0.27	0.24	18.7	0.04	5.7	6.1	366	n.d.	137	2.7	53	26	2
17	38.2	22.0	8.08	0.31	0.47	0.22	26.1	0.05	16.9	3.1	300	″	160	1.2	46	40	3
18	53.0	25.9	3.92	0.13	0.31	0.45	7.43	0.06	3.7	3.5	104	11	40.7	3	30	22	2
*	0.01		1^{-4}	1^{-4}	5^{-4}	2^{-3}	5^{-5}	1^{-4}	2^{-3}	0.4	1	4	0.1	0.1	3	5	2

Note: (1–3, 5–11, 14) Pyrite–pyrrhotite ore; (4, 2, 13, 15) chalcopyrite–pyrite–pyrrhotite ore; (16–18) sulfoarsenide–sulfide ore. Samples were analyzed at the Laboratory of Activation (Canada); * is the detection limit. Fe, S, Cu, Co, Cr, Ni, As, and Mn contents are given in wt %; other elements, in ppm. Cd was detected in samples 1, 13, 14, and 17 (1.6, 1.6, 2.7, and 0.6 ppm, respectively; the detection limit is 0.5 ppm.

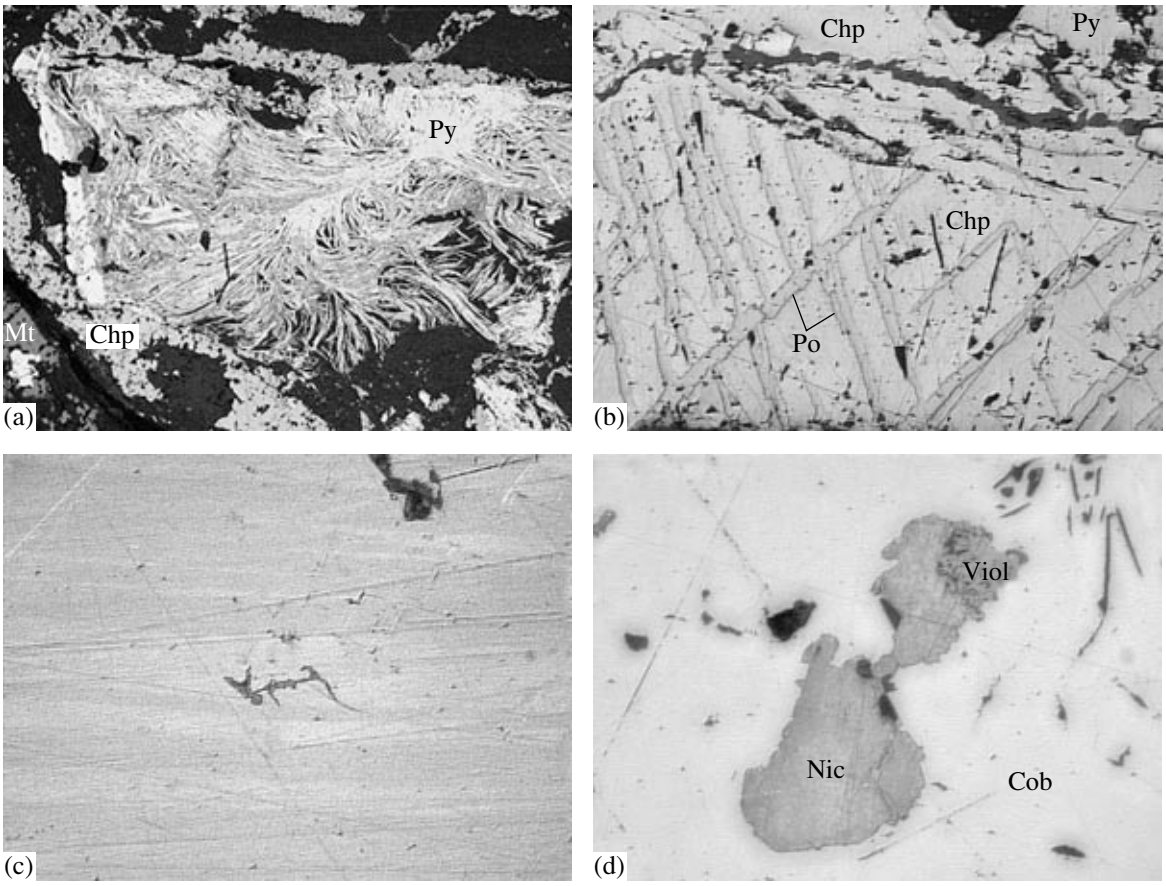

Fig. 6. Structure of sulfides from the Ishkinino deposit. (a) Fibrous structure of serpentinite in an intergrowth with pyrite II, 1.2 mm, sample 610-1a; (b) pyrrhotite lamellas in chalcopyrite, 0.79 mm, sample 15; (c) wormlike inclusion of mackinawite in chalcopyrite with polysynthetic twins; black is a defect of polishing, polars are slightly crossed, 0.38 mm, sample 335; (d) violarite–polydymite replacing nickeline, 0.79 mm, sample 610-21a. (Py) pyrite, (Chp) chalcopyrite, (Po) pyrrhotite, (Mc) marcasite, (Sph) sphalerite, (Viol) violarite, (Cob) cobaltite, (Ars) arsenopyrite, (Gers) gersdorffite, (Nic) nickeline, (Cr) chromite, (Mt) magnetite, (Au) gold. Figs. 6–9 and 12 (except Fig. 8d) are photomicrographs of polished sections in reflected light; sizes in millimeters are the natural widths of microphotographs.

MINERALOGY OF ORE

Twenty-three ore minerals have been identified in ore at the Ishkinino deposit. The major minerals include pyrrhotite, pyrite, and chalcopyrite; magnetite, chromite, arsenopyrite, cobaltite, gersdorffite, nickeline, marcasite, pentlandite, mackinawite, and minerals of the linnaeite group (four varieties) are second in abundance, and loellingite, safflorite, rammelsbergite, krutovite, native gold, sphalerite, and rucklidgeite are rare minerals (Melekestseva and Zaikov, 2003).

Sulfides

Pyrrhotite is represented by hexagonal and monoclinic polymorphs that include four generations and numerous morphological varieties: coarse- and fine-grained, tabular, granular, and veined.

Pyrite is represented by three generations and several morphological varieties. Pyrite together with *marcasite* replaces pyrrotite, making up a bird's-eye ore; forms veins consisting of large subhedral crystals; and occurs as concentrically zoned and colloform aggregates in sandstones. Pyrite–serpentine intergrowths have a peculiar fibrous structure (Fig. 6a).

The chemical compositions of pyrrhotite and pyrite correspond to $Fe_{0.86}S$ and $Fe_{0.98}S_2$, respectively. Various generations of pyrrhotite and pyrite are distinguished by Ni contents (Table 4); the late pyrrhotite III and pyrite III are the most enriched in Ni (up to 0.35 and 0.51 wt %, respectively).

Chalcopyrite is a later mineral with respect to pyrrhotite I and pyrite I. The allotriomorphic granular structure of chalcopyrite aggregates is the most abundant. The mineral is represented by several generations indistinguishable from one another in morphology and chemistry. A latticed structure with oriented pyrrhotite lamellas is often observed (Fig. 6b). The chemical composition of chalcopyrite $Cu_{0.94}Fe_{0.99}S_2$ fits the theoretical composition with insignificant deviations from stoichiometry (Table 4).

Table 4. Chemical composition of sulfides from the Ishkinino deposit, wt %

No.	Sample	Fe	Cu	S	Ni	Co	As	Total
				Pyrrhotite I, II				
1	2	60.58	–	40.88	0.04	n.a.	n.a.	101.50
2	2	61.11	–	41.22	0.17	″	0.01	102.51
3	2	60.66	–	41.57	0.03	0.04	n.a.	102.30
				Pyrrhotite III				
4	1	60.43	–	39.79	0.24	0.02	0.03	100.51
5	1	60.45	–	40.05	0.35	0.01	0.01	100.87
				Pyrite I				
6	2	46.64	–	54.85	0.12	0.03	0.04	101.68
7	2	46.45	–	54.84	0.32	0.00	n.a.	101.64
8	2	45.71	–	54.55	0.41	0.00	″	100.67
				Pyrite II				
9	1	47.27	–	53.35	0.02	0.01	0.01	100.66
10	1	46.97	–	53.93	0.08	0.01	n.a.	100.99
				Pyrite III				
11	1	46.77	–	54.14	0.51	0.09	0.02	101.53
12	1	47.15	–	52.50	0.45	0.02	0.08	100.20
13	1	47.99	–	50.84	0.33	0.01	n.a.	99.17
				Chalcopyrite				
14	610-21b	30.36	34.42	35.12	n.a.	n.a.	n.a.	99.93
15	610-21b	30.91	32.89	35.73	0.26	0.01	0.02	99.81
16	610-21b	31.60	32.29	35.44	0.42	0.02	0.02	99.83
17	610-21b	30.56	34.16	34.80	0.06	0.01	n.a.	99.60
				Pentlandite				
18	610-21b	18.11	0.79	40.26	35.05	3.77	0.02	98.00
19	610-21b	16.59	0.27	40.95	36.73	3.77	0.03	98.34
20	610-21b	15.85	0.69	41.13	37.99	3.06	0.01	98.73
				Violarite-1				
21	598-15	26.69	n.a.	41.33	29.77	0.37	n.a.	98.16
22	598-15	28.65	″	41.68	27.29	1.39	″	99.01
23	4	22.73	″	40.91	34.08	0.56	″	98.28
24	4	22.75	″	40.97	33.95	0.72	0.02	98.41
				Violarite-3				
25	610-21a	51.88	0.52	42.26	3.21	0.22	0.01	98.10
26	598-15	41.14	n.a.	43.42	13.26	0.16	0.04	98.02
27	610-21b	47.64	0.60	40.38	9.35	0.07	n.a.	98.08
28	598-18b	37.68	n.a.	42.58	18.53	0.14	0.01	98.95
				Violarite-4				
29	15	15.85	n.a.	39.62	26.40	16.32	0.04	98.23
30c	15	14.56	″	41.57	24.86	17.68	0.03	98.70
31r	15	18.24	″	39.34	25.65	15.15	n.a.	98.38
32c	15	11.95	″	42.28	29.65	16.53	″	100.41
33r	610-21b	19.29	″	41.87	23.43	14.42	0.03	99.04

Note: Zonal grains of violarite-4: (c) core, (r) rim. Analyses were performed on a JEOL JXA-8900RL microprobe at the Freiberg Mining Academy, Germany, analyst K. Becker. Here and hereafter, n.a. denotes not analyzed.

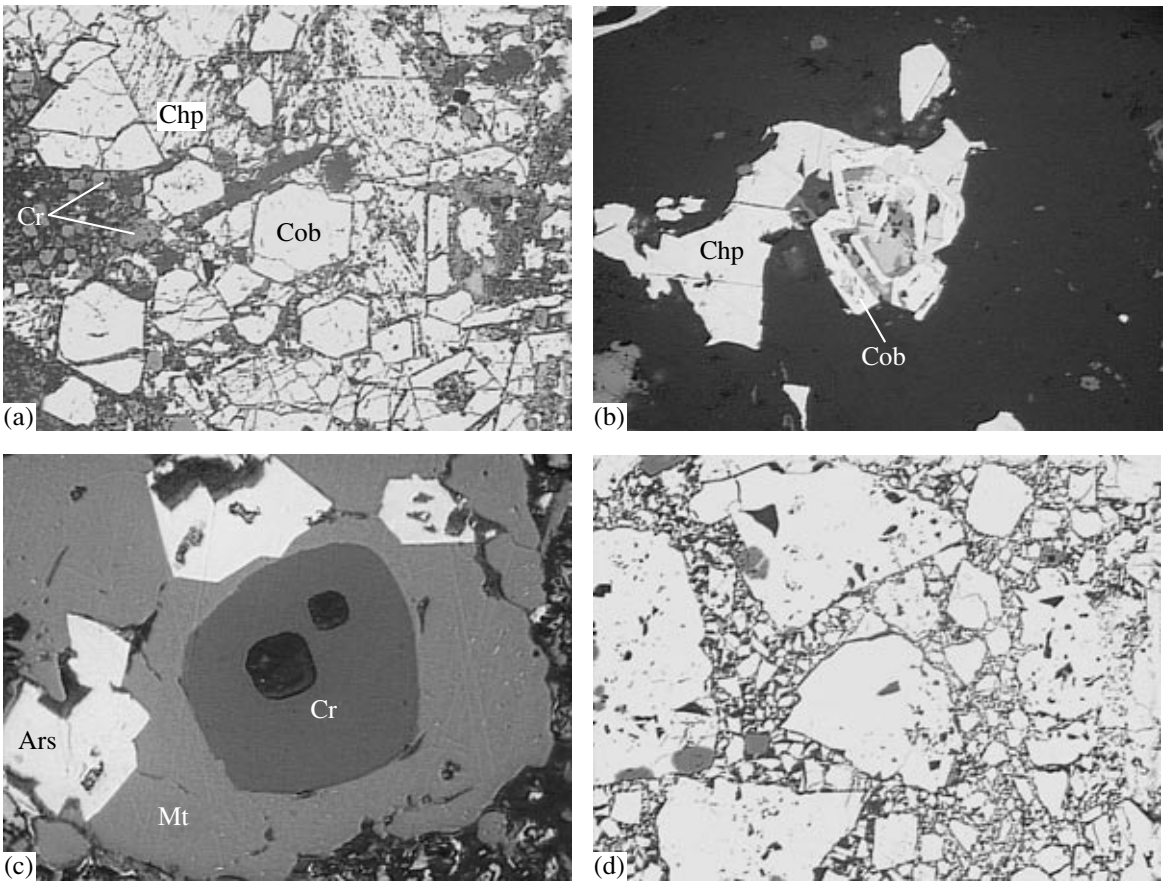

Fig. 7. Co and Fe sulfoarsenides from the Ishkinino deposit. (a) Aggregate of cobaltite and chromite crystals in chalcopyrite, 3 mm, sample 610-21a; (b) cobaltine crystal, black is serpentine, 0.38 mm, sample 342C; (c) intergrowths of arsenopyrite crystals in magnetite that replaced chromite, 0.16 mm, sample 5; (d) cataclastic structure of arsenopyrite aggregates in ore of sulfoarsenide–sulfide type, gray euhedral grains are chromite, 3 mm, sample 598-17.

Chalcopyrite aggregates occasionally contain skeletal (star-shaped) *sphalerite* crystals as products of exsolution of Zn-bearing chalcopyrite solid solution at ~350°C (Kostov and Minčeva-Stefanova, 1981).

Pentlandite occurs as tabular aggregates in pyrrhotite I and is commonly replaced with violarite. Flamelike aggregates of pentlandite confined to former cleavage fractures in pyrrhotite are retained in chalcopyrite that replaced pyrrhotite. These aggregates mark the breakdown of pentlandite–pyrrhotite solid solution, which is completed at ~150°C (Kostov and Minčeva-Stefanova, 1981). The chemical composition of pentlandite $(Ni_{3.94}Fe_{1.88}Co_{0.38})_{6.20}S_8$ is characterized by a great deficiency in metals (Table 4).

Mackinawite occurs in chalcopyrite grains as small flakes, lamellas, and worm- and threadlike inclusions (Fig. 6c) no larger than 20–30 μm across. Relict pentlandite replaced with mackinawite is occasionally retained within chalcopyrite grains.

Minerals of the linnaeite group are represented by four varieties different in composition. *Violarite-1* occurs as lamellas (up to 15–20 μm in size) in chalcopyrite and has a smooth surface without fractures. The composition of this variety $(Fe_{1.58}Ni_{1.49}Co_{0.03})_{3.10}S_4$]–[$(Ni_{1.81}Fe_{1.28}Co_{0.03})_{3.12}S_4$ (Table 4) is close to the theoretical composition of violarite.

Violarite-2 replaces nickeline grains as a microgranular aggregate (Fig. 6d). Its composition $(Ni_{2.20}Fe_{0.66}Co_{0.06})_{2.92}(S_{3.94}As_{0.06})_{4.00}$ falls into the region of intermediate members of the violarite–polydymite isomorphic series, while the elevated Ni and As contents (≥1 wt %) are inherited from the replaced nickeline.

Violarite-3 was detected in chalcopyrite as very thin (up to 3 μm), pinkish lilac, blinking and broken lamellas. Fe prevails over Ni in its composition, and Co is present in insignificant amounts (Table 4). The chemical composition $(Fe_{1.94}Ni_{0.93})_{2.87}S_4$]–[$(Fe_{2.82}Ni_{0.15}Cu_{0.03})_{3.00}S_4$ is intermediate between violarite and greigite.

Violarite-4 was identified as fractured fine-grained aggregates (as large as 0.13–0.15 mm) that replace pentlandite and pyrrhotite. The mineral is markedly enriched in Co (up to 18.39 wt %, see Table 4) relative to other varieties. The composition of this mineral $(Ni_{1.29}Co_{0.92}Fe_{0.80})_{3.01}S_4$]–[$(Ni_{1.22}Fe_{1.07}Co_{0.73})_{3.02}S_4$ is transitional between violarite and siegenite. The high Co contents testify to the replacement of cobalt pent-

Table 5. Chemical composition of Co, Ni, and Fe sulfoarsenides from the Ishkinino deposit, wt %

No.	Sample	As	S	Co	Ni	Fe	Bi	Total
				Cobaltite				
1	610-21A	46.36	18.45	15.17	14.69	5.72	0.22	100.41
2	610-21	47.09	18.07	24.94	7.00	3.72	0.25	100.82
3		48.30	17.36	23.53	8.37	3.38	0.01	100.93
4		47.10	17.70	21.36	9.51	4.45	0.00	100.11
5		47.14	18.23	18.18	11.83	5.50	0.02	100.87
6		46.69	18.33	19.35	11.66	5.00	0.19	101.02
7		47.20	18.20	15.76	13.82	6.25	0.12	101.23
8		47.02	18.31	20.23	10.46	5.18	0.09	101.19
9		46.96	18.60	23.37	7.87	4.61	0.04	101.40
10	610-21A	44.14	20.02	29.94	3.95	3.04	0.01	101.10
11		45.40	19.11	16.88	14.40	5.86	0.01	101.88
				Arsenopyrite				
12	610-22	50.68	16.42	0.67	7.20	26.33	0.00	101.51
13		51.84	15.18	2.68	8.89	22.18	0.00	100.77
14		57.97	10.76	2.65	14.66	15.02	0.00	101.17
15		54.96	12.94	2.88	11.62	18.53	0.11	101.28
16	598-16	47.71	18.36	1.55	4.89	28.88	n.a.	101.40
17		48.26	17.77	4.27	3.08	28.06	″	101.45
18		48.82	16.90	1.92	6.11	26.65	″	100.39
19		46.31	19.16	3.77	2.03	29.91	″	101.18
				Gersdorffite				
20	610-22	50.23	16.42	2.88	20.07	11.30	n.a.	101.73
21		51.33	15.62	2.16	20.16	11.69	″	101.70
22	I-105-2c	46.31	17.25	10.48	16.73	8.44	″	99.21
23		46.90	16.66	6.26	19.81	9.00	″	98.63
24		45.67	17.16	12.18	16.26	7.87	″	99.13
25		47.86	17.33	11.72	17.22	7.31	″	101.43
26		46.68	16.97	9.36	19.49	7.03	″	99.53
27		44.99	17.74	12.68	15.55	7.65	″	98.61

Note: Samples 1–9, 12–15, 20, and 21 were analyzed on a Camebax SX 50 microprobe at the Museum of Natural History, London, analyst J. Spratt; samples 10, 11, 16–19, on a JEOL JXA-8900RL microprobe at the Freiberg Mining Academy, Germany, analyst K. Becker; samples 22–27, on a JEOL JCXA-733 at the Institute of Mineralogy, Uralian Division, Russian Academy of Sciences, analyst E.I. Churin.

landite with this mineral (Borishanskaya et al., 1981). It was established that the grains of violarite-4 reveal a slightly expressed zoning. The inner zone is characterized by enrichment in Co and depletion in Fe, whereas opposite proportions are typical of the outer zone. In some cases, Ni is correlated with Fe and mimics the zonal distribution of the latter, while in other cases Fe is correlated with Co.

Sulfoarsenides

Cobaltite forms segregations in carbonate veins that cut the sulfide matrix (Fig. 7a) and occurs among sulfides as separate cubic and octahedral crystals 0.1–2.0 mm in size as well as intergrowths. Sheath crystals (Fig. 7b) are abundant. Cobaltite $(Co_{0.43}Ni_{0.42}Fe_{0.17})_{1.02}As_{1.03}S_{0.97}$ is distinguished by high (up to 14.69 wt %) Ni content (Table 5). All cobaltite crystals reveal a zonal distribution of Co and Ni. Elevated Co contents (as high as 29.14 wt %) are detected in the cores of crystals $(Co_{0.84}Ni_{0.12}Fe_{0.08})_{1.04}As_{0.98}S_{1.02}$, while elevated Ni contents are typical of the outer zones (conditionally direct zoning). Reverse and oscillating zoning are also observed.

Arsenopyrite is represented by two morphological varieties: small (~0.04 mm) rhombic crystals and their

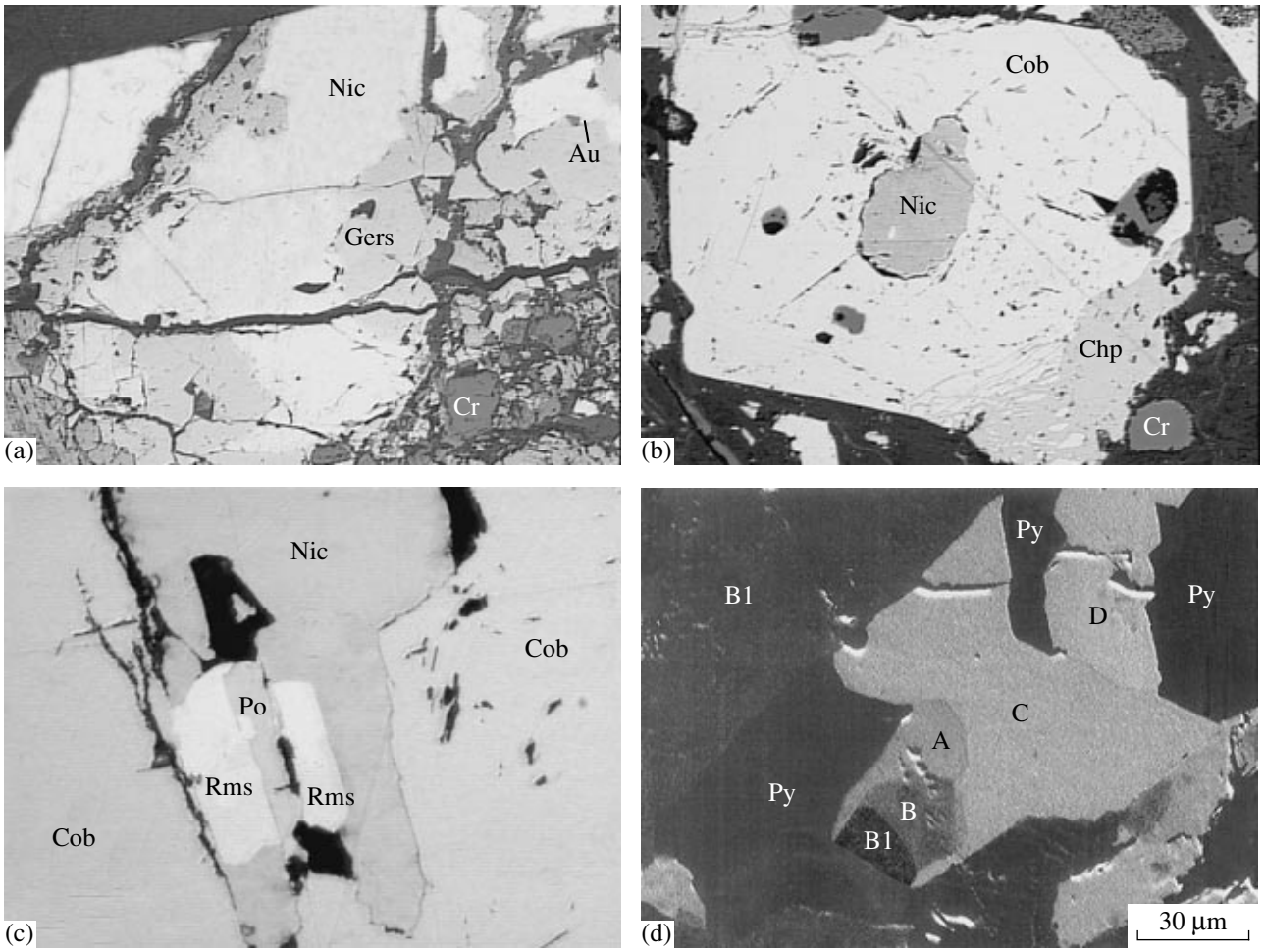

Fig. 8. Ni sulfoarsenides and Co, Ni, and Fe arsenides from the Ishkinino deposit. (a) Coarse-grained gersdorffite and nickeline aggregates, 3 mm, sample I-105-2; (b) nickeline in cobaltite crystal, black is serpentine, 0.79 mm, sample 610-B; (c) cobaltite with relics of rammelsbergite (Rms) of tabular habit, nickeline, and pyrrhotite, 0.16 mm, sample 610-B; (d) fragment of intergrowth of As-bearing minerals in pyrite crystal: (A) krutovite, (B) gersdorffite, (B1) cobaltite, (C) nickeline, (D) rammelsbergite, sample 610-C; BSE image made on a Camscan-4DV SEM equipped with an AN-10000 energy dispersive X-ray spectrometer at the PC+ Company, St. Petersburg, analyst Yu.L. Kretser.

intergrowths in ore and the lithic matrix (Fig. 7c) and veins consisting of large (a few millimeters) cataclastic grains (Fig. 7d). The zonal distribution of Ni and Co in arsenopyrite grains is notable. A phase transitional between arsenopyrite and gersdorffite was revealed with microprobe (Table 5, an. 14, 16). The anomalously high Ni content (up to 14.66 wt %) established in arsenopyrite is untypical of this mineral (Borishanskaya et al., 1981).

Gersdorffite forms coarse-grained crystalline aggregates (up to 0.5–1.0 mm in size) in association with nickeline (Fig. 8a) occurs as individual crystals (Fig. 9b), and also as a relic in cobaltite together with arsenides. The mineral is enriched in Co (up to 13 wt %), fitting the formula $(Ni_{0.45}Co_{0.38}Fe_{0.24})_{1.07}As_{1.04}S_{0.96}$, and in Fe (11 wt %), fitting the formula $(Ni_{0.58}Fe_{0.36}Co_{0.07})_{1.01}As_{1.17}S_{0.83}$ (Table 5). The gersdorffite grains are zonal owing to the variable contents of these elements. The Co content increases inward up to 12–13 wt % and the Fe content decreases in the same direction down to 7–8 wt %. Conversely, the outer zone is depleted in Co (6 wt %) and enriched in Fe (9 wt %).

Arsenides

This group of minerals comprises mono- and diarsenides. Monoarsenides are represented by *nickeline* as tabular grains and allotriomorphic granular aggregates as large as 3 mm across. Nickeline is associated with cobaltite and gersdorffite, occurring as inclusions in these minerals (Fig. 8b) and observed as large aggregates together with gersdorffite (Fig. 8a). The chemical composition of nickeline fits the formula $(Ni_{0.99–1.01}Co_{0.01})_{1.00–1.01}As_{1.00}$ (Table 6).

Only nickeline NiAs and skutterudite $CoAs_3$ were previously noted as Co, Ni, and Fe arsenides at the massive sulfide deposits in the Urals. While studying the

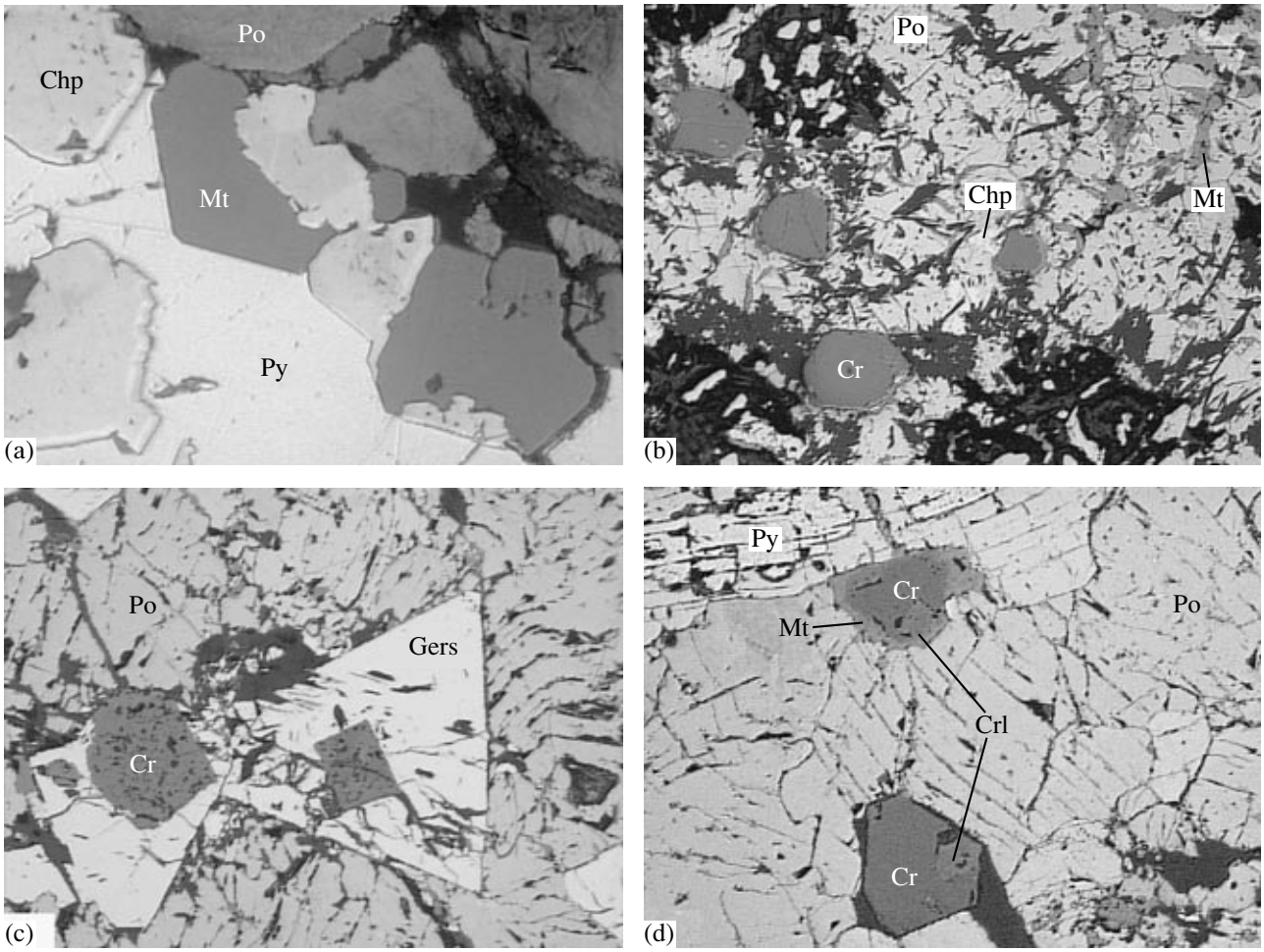

Fig. 9. Oxides in ore of the Ishkinino deposit. (a) Magnetite replaced with chalcopyrite pseudomorph in selvage of pyrite vein, 0.16 mm, sample 4; (b) chromite in pyrite–pyrrhotite ore, black is serpentine, 0.79 mm, sample 337; (c) chromite with corroded surface in gersdorffite crystals (0.79 mm), sample I-105-2c; (d) chromites with magnetite rims and ore inclusions (Cr1), 0.79 mm, sample 2.

ore at the Ishkinino deposit, we also identified *loellingite* $FeAs_2$, *safflorite* $(Co,Fe)As_2$, *rammelsbergite* $NiAs_2$, and *krutovite* $NiAs_2$, which were previously unknown from the massive sulfide ore in the Urals. These minerals have been detected within cobaltite crystals as tabular and xenomorphic grains from 2–3 to 50 μm in size (Fig. 8c) that replace nickeline and gersdorffite. Rammelsbergite and krutovite also occur within nickeline. Safflorite commonly grows over nickeline along the crystal margins; krutovite is occasionally associated with loellingite. Sporadic allotriomorphic granular aggregates of closely intergrown diarsenides, nickeline, and gersdorffite up to 100 μm in size are shown in Fig. 8d.

Loellingite and safflorite are enriched in Ni up to 11 and 10 wt %, respectively. The results of analysis are recalculated to the formulas $(Fe_{0.50}Ni_{0.40}Co_{0.13})_{1.03}(As_{1.96}S_{0.04})_{2.00}$ and $(Co_{0.58}Ni_{0.31}Fe_{0.16})_{1.05}(As_{1.27}S_{0.73})_{2.00}$. Safflorite $(Co_{0.83}Ni_{0.19}Fe_{0.06})_{1.08}As_{2.00}$ also contains up to 13 wt % S. Rammelsbergite $(Ni_{0.57}Co_{0.41}Fe_{0.06})_{1.04}(As_{1.96}S_{0.04})_{2.00}$ contains up to 12 wt % Co. Up to 8 wt % S content was established in krutovite $(Ni_{0.80}Co_{0.13}Fe_{0.06})_{0.99}(As_{1.51}S_{0.49})_{2.00}$, corresponding to a transitional member of the krutovite–gersdorffite isomorphic series (Borishanskaya et al., 1981). Up to 1 wt % Bi was revealed in rammelsbergite and krutovite (Table 6).

Tellurides

A telluride of Bi and Pb was detected by S.G. Tesalina in association with arsenides as grains a few micrometers in size. The mineral consists of 31.40 wt % Te, 41.19 wt % Bi, and 2.82 wt % Pb. The proportions of elements suggest that this mineral is *rucklidgeite* $(Bi, Pb)_3Te_4$.

Oxides

Magnetite is represented by three generations and two morphological varieties. The first variety forms veinlets and xenomorphic aggregates that replace pyr-

Table 6. Chemical composition of Co, Ni, and Fe arsenides from the Ishkinino deposit, wt %

No.	Sample	As	S	Co	Ni	Fe	Bi	Total
				Nickeline				
1	610-21	56.44	0.13	0.69	43.47	0.16	0.18	101.47
2		56.44	0.14	0.76	43.63	0.16	0.22	101.55
				Loellingite				
3	Ish-41	70.38	0.91	2.35	9.94	15.71	0.13	99.64
4		70.57	0.77	3.44	11.12	13.82	0.08	100.03
5		69.51	1.83	4.14	10.82	14.05	0.09	100.55
				Safflorite				
6		71.42	0.11	22.38	5.15	1.52	n.a.	100.81
7		52.74	12.77	17.97	10.08	4.47	″	98.04
8		71.42	0.42	25.44	2.26	1.20	0.02	100.76
				Rammelsbergite				
9		70.06	1.14	2.85	25.05	1.11	n.a.	100.78
10		67.85	0.99	7.64	22.43	1.34	″	100.42
11	610-B	71.70	0.55	12.08	16.15	1.49	0.25	102.30
12		71.82	0.42	11.91	15.45	1.75	0.00	101.35
13	610-C	70.99	0.55	7.97	13.82	6.35	0.00	99.84
14		70.39	1.12	4.52	23.68	0.84	0.97	101.77
				Krutovite				
15	Ish-41	60.82	7.89	5.03	24.67	1.46	n.a.	100.10
16		61.31	7.84	3.64	25.60	2.14	″	101.80
17		60.54	8.27	3.98	25.41	1.65	″	100.43
18		65.78	4.30	1.96	27.30	0.65	″	100.52
19	610-C	60.50	7.12	4.62	25.65	1.04	0.43	99.37
20		62.79	6.51	4.37	26.14	0.80	0.53	101.13
21		62.25	6.84	5.48	24.83	0.98	0.45	100.82

Note: Samples 1, 2, 3–7, and 12–15 were analyzed on a Camebax SX 50 microprobe at the Museum of Natural History, London, analyst J. Spratt; samples 8–11 and 16–21, on a Camscan-4DV SEM equipped with an AN-10000 energy dispersive X-ray spectrometer at the PC+ Company, St. Petersburg, analyst Yu.L. Kretser.

rhotite, pentlandite, violarite, chromite, pyrite, and chalcopyrite. The anhedral crystals in selvages of veins composed of pyrite II and quartz (Fig. 9a) are regarded as the second variety. Magnetite is stable in chemical composition (Table 7), and only when replacing chromite does magnetite become enriched in Cr_2O_3 up to 3.15 wt %.

Chromite is distributed noniniformly through the ore but occurs in all ore types. Chromite and chromite–cobaltite segregations are often hosted in the chlorite–serpentinite matrix (Fig. 7a). Chromite is represented by euhedral octahedral crystals often replaced with magnetite (Fig. 9b). Some grains are rounded and their surface is corroded (Fig. 9c) and broken by cracks. Chromite grains sporadically contain pyrite and chalcopyrite confined to growth zones, and chromite itself occasionally occurs at growth zones of cobaltite. Rounded, isometric, and oblong one-, two, and three-phase mineral and melt inclusions are noted (Fig. 7c). They are commonly composed of ortho- and clinopyroxene and glass (Tesalina et al., 2003). Tabular ore inclusions with elevated reflectivity in comparison with chromite are often observed within chromite crystals and at their margins (Fig. 9d).

The following compositional variations in chromites were established: 48.32–53.65 wt % Cr_2O_3, 21–31 wt % FeO, 11.14–13.91 wt % Al_2O_3, and 5.20–9.91 wt % MgO (Table 7). Chromite grains incorporated into cobaltite crystals are enriched in NiO and CoO (0.10 and 0.23 wt %, respectively). The lighter ore inclusions are characterized by approximately equal Cr_2O_3 and FeO contents: 48.01 and 46.35 wt %, respectively.

Native Elements

Native gold is associated with As-bearing minerals. Numerous gold grains occur in cobaltite, arsenopyrite, gersdorffite, nickeline, and safflorite. Native gold is

Table 7. Chemical composition of oxides from the Ishkinino deposit, wt %

No.	Sample	Cr_2O_3	FeO	Al_2O_3	MgO	TiO_2	MnO	V_2O_3	NiO	CoO	Total
					Chromite						
1	2	51.95	26.56	12.27	7.98	0.26	0.36	0.28	0.06	0.05	99.77
2		52.80	25.92	10.68	7.94	0.24	0.38	0.27	0.04	0.02	98.29
3	4a	49.56	29.98	11.74	6.44	0.28	0.42	0.27	0.02	0.05	98.76
4		51.86	24.50	13.39	9.17	0.33	0.33	0.30	0.06	0.00	99.94
5	610-21b	48.84	29.53	12.05	6.68	0.39	0.40	0.28	0.06	0.06	98.29
6		48.65	33.06	12.17	5.40	0.40	0.38	0.32	0.05	0.07	100.50
7	610-1a	51.68	27.82	11.46	6.90	0.22	0.40	0.22	0.06	0.02	98.78
8		52.33	28.33	10.84	6.15	0.32	0.41	0.28	0.08	0.04	98.78
9	15	53.44	21.66	13.38	10.28	0.25	0.37	0.18	0.01	0.00	99.57
10		52.83	22.16	12.95	10.28	0.23	0.32	0.20	0.06	0.00	99.03
11		49.38	23.66	18.15	8.02	0.30	0.34	0.21	0.05	0.03	100.14
12		53.90	21.93	14.05	10.10	0.24	0.29	0.18	0.01	0.01	100.71
13	610-21a	50.59	28.68	12.10	8.26	0.35	0.39	0.32	0.07	0.07	100.83
14		51.94	24.87	13.06	9.69	0.35	0.35	0.12	0.06	0.06	100.50
15		48.11	35.63	10.97	4.10	0.44	0.44	0.30	0.11	0.31	100.41
16		46.92	33.69	13.54	5.28	0.22	0.33	0.33	0.11	0.35	100.77
17		48.51	31.10	11.63	5.50	0.27	0.49	0.28	0.12	0.26	98.16
18		47.42	32.48	12.33	5.32	0.26	0.37	0.27	0.17	0.42	99.04
19	610-1a	54.34	25.73	11.02	8.28	0.21	0.32	0.30	0.05	0.04	100.29
20		53.50	28.47	12.50	6.39	0.37	0.34	0.17	0.04	0.01	101.79
21	610-21b	47.58	31.53	12.73	5.48	0.34	0.35	0.39	0.06	0.08	98.54
22		49.78	31.71	12.38	5.52	0.36	0.30	0.33	0.06	0.06	100.50
23	15	43.67	53.60	0.77	1.05	0.61	0.54	0.29	0.01	0.00	100.54
24		48.56	43.26	2.34	3.05	0.29	0.44	0.27	0.09	0.00	98.30
25		53.58	40.75	1.50	1.77	0.52	0.46	0.38	0.02	0.03	99.01
					Magnetite						
26	610-1a	0.00	99.70	0.00	0.07	0.00	0.11	0.02	0.00	0.00	99.90
27		0.05	99.53	0.02	0.12	0.03	0.10	0.00	0.01	0.00	99.86
28	15	1.94	97.34	0.00	0.17	0.00	0.16	0.02	0.00	0.00	99.63
29	4a	3.15	94.59	0.01	0.26	0.05	0.20	0.04	0.00	0.00	98.30
30		2.80	95.40	0.00	0.28	0.01	0.26	0.02	0.00	0.00	98.77

Note: (1, 2) Chromite from pyrite–pyrrhotite ore; (3–8) chromite from chalcopyrite–pyrite–pyrrhotite ore; (9–18) chromite from sulfoarsenide–sulfide ore, including (15–18) chromite within cobaltite crystals; (19–22) chromite from serpentinite in ore; (23–25) ore inclusions in chromite. Analyses were performed on a JEOL JCXA-733 at the Institute of Mineralogy, Uralian Division, Russian Academy of Sciences, analyst E.I. Churin.

observed as rounded, triangular, and xenomorphic grains attaining 70 μm in size. Sporadic anhedral and euhedral gold grains as large as 30 μm were found in pyrrhotite and chalcopyrite. All gold grains contain 16–23 wt % Ag. The Au/Ag ratio in native gold associated with sulfoarsenides and arsenides varies from 3 : 1 to 4 : 1. Gold grains intergrown with sulfides contain less silver and the Au/Ag ratio equals (4 : 1)–(6 : 1).

On the basis of structural features and microscopic examination, the ore minerals were divided into four progressively formed mineral assemblages (1–4 are mineral assemblages and I–IV are generations of minerals): (1) pyrrhotite I and pentlandite ⟶ pyrrhotite II, pyrite I, and magnetite I ⟶ (2) chalcopyrite I, sphalerite, and gold? ⟶ (3) nickeline ⟶ gersdorffite ⟶ loellingite, safflorite, rammelsbergite, krutovite, rucklidgeite, and gold ⟶ cobaltite and arsenopyrite ⟶ (4) magnetite II ⟶ pyrite II, chalcopyrite II, minerals of the linneaite group, and pyrrhotite III ⟶ pyrite III and pyrrhotite IV ⟶ magnetite III.

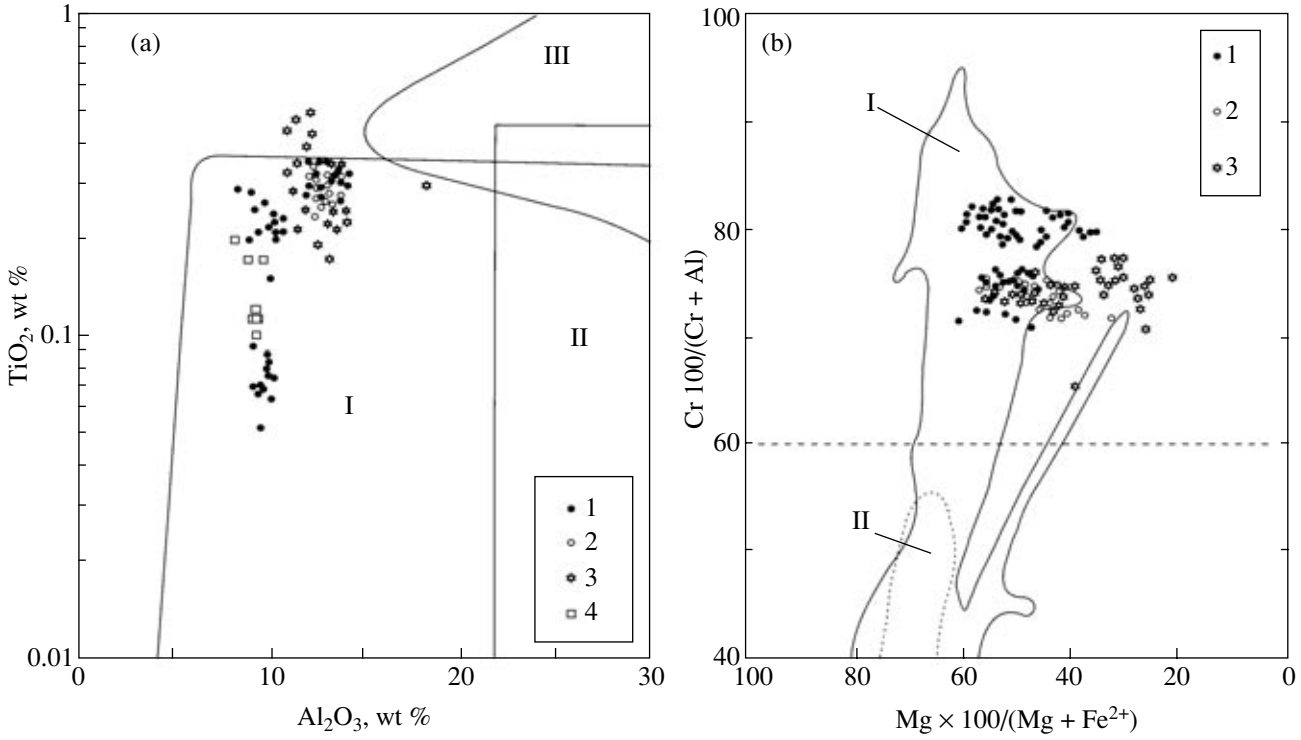

Fig. 10. Compositions of chromite plotted on classification diagrams. (1–4) Chromites from (1) serpentinite, (2) serpentinite mass in ore, (3) massive sulfide ore, and (4) dikes of high-Mg andesite, after P. Jonas. (a) Contours of fields (Kamenetsky et al., 2001): (I) peridotites of suprasubduction zones, (II) peridotites of mid-ocean ridges, (III) MORB; (b) contours of fields (Dick and Bullen, 1984): (I) Alpine-type ultramafic rocks, (II) peridotites of mid-ocean ridges.

DISCUSSION

The deposits located in the MUFZ were suggested to be related to gabbroic rocks (Subbotin), ultramafic rocks (Buchkovsky, 1970), or Early Silurian basalts (Zakharov and Zakharova, 1969). Currently, many researchers refer them to the Cyprus type of massive sulfide deposits (Kontar and Libarova, 1997, among others).

Our investigations have shown that the process of ore formation was rather complex. The repeated deformation and redistribution of ore matter made it possible to establish the subduction- and collision-related stages in the formation of the Ishkinino deposit. The geological history of the deposit was reconstructed taking into account the structure and geodynamics of the MUFZ and the results of study of the similar Ivanovka and Dergamysh deposits.

Development of the ore-bearing structure. Geological, geochemical, and mineralogical data on the ore field indicate that the stratified rocks were formed in two settings: oceanic (Sakmara Formation) and island-arc (Baimak–Buribai Formation). The former are geochemically akin to oceanic basalts, while the latter are close to boninites from island arcs.

As follows from chromite compositions (Dick and Bullen, 1984; *Metallogeny*…, 1999; Kamenetsky et al., 2001), the ultramafic rocks are also characterized by island-arc attributes (Tesalina et al., 2003; Dunaev and Churin, 2003). Chromites with Cr # > 60% fall into the fields of suprasubduction peridotites and island-arc basalts (Figs. 10a, 10b). Chromites from dikes of high-Mg andesites also fall into these fields (Jonas, 2003). The high Cr # is regarded as independent evidence for strong depletion of peridotites belonging to the harzburgite association as the most typical rocks of island-arc ultramafics (Dick and Bullen, 1984; *Metallogeny*…, 1999; Kamenetsky et al., 2001).

In present-day geodynamic settings, the intimate combination of ultramafic sheets and oceanic and island-arc volcanics is revealed only in the accretionary prisms of the active island arcs (*Metallogeny*…, 1999).

The collision that began in the Late Devonian (Puchkov, 2000) resulted in the formation of the antiform that characterizes the present-day structure of the ore field. It has been established that thrusting and strike-slip dislocations caused by oblique displacements accompanied the collision (Seravkin et al., 2003). Such near-meridional strike-slip faults have been documented in the Ishkinino ore field, where they bound the suture zone in the east.

Age of ore mineralization. On the basis of graptolites found in the ore-bearing sequence, it was previously accepted that the cobalt–copper massive sulfide deposits were formed in the Silurian (Zakharov and

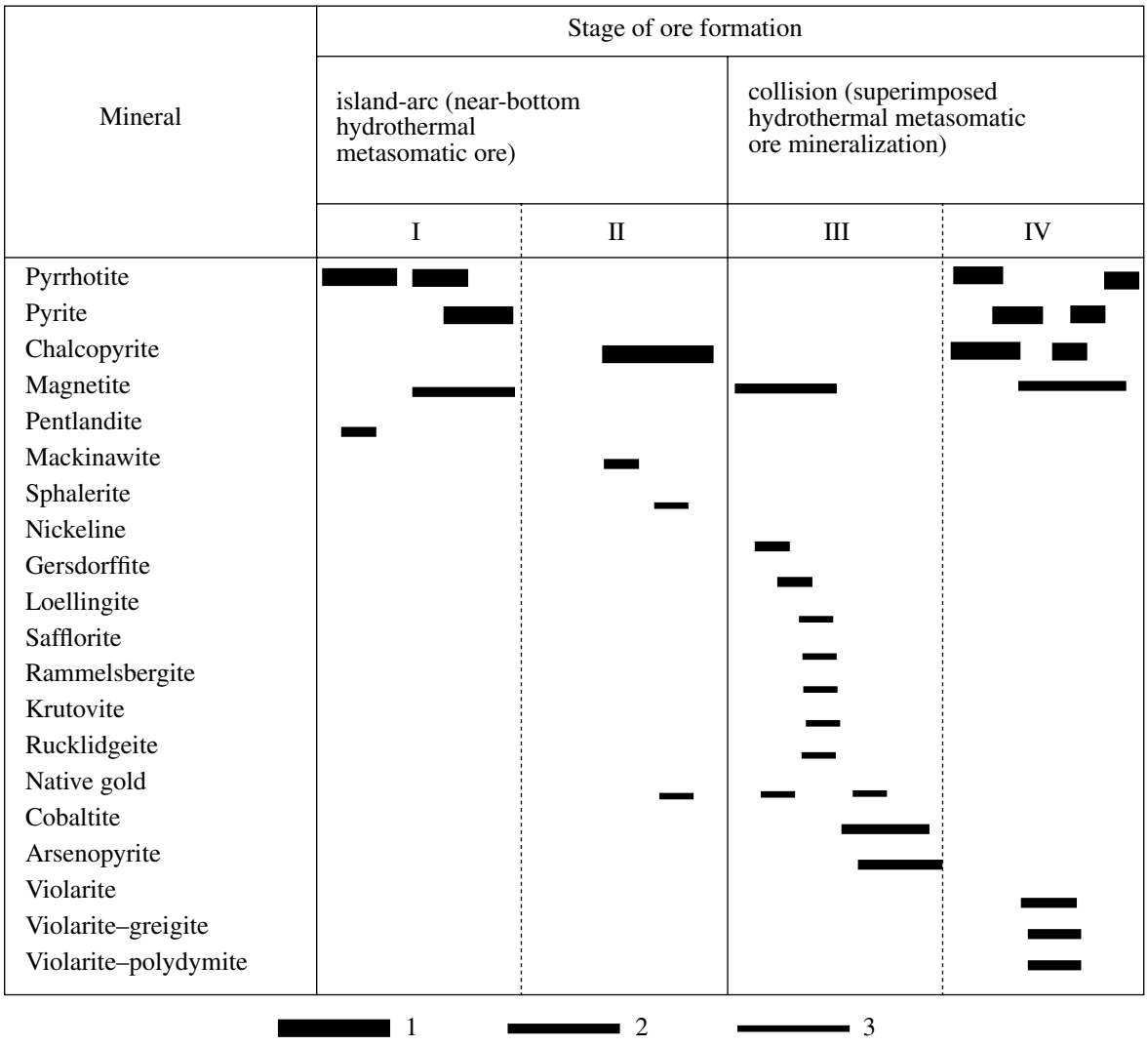

Fig. 11. Formation sequence of hypogene ore minerals at the Ishkinino deposit. (I–IV) Mineral assemblages; (1–3) ore minerals: (1) major, (2) second in abundance, (3) rare. The relict chromite from ultramafic rocks is not shown.

Zakharova, 1969). At present, it has been established that the graptolites were found in large olistoliths as constituents of olistostrome, whereas Middle Devonian conodonts are contained in the matrix (Seravkin et al., 2003). Furthermore, many orebodies at the Ivanovka deposit are hosted in basaltic rocks, the oceanic affinity of which has not been confirmed; they have calc-alkaline signatures, and some of them are similar to boninites (Simonov et al., 2002).

As concerns the Ishkinino deposit, it has been established that the ore was formed in the ultramafic rocks before the onset of andesitic basaltic volcanic activity. The Silurian sedimentary rocks of the Sakmara Formation do not contain ultramafic clastic material or chromites. This implies that, during the formation of the Silurian ophiolitic association, the ultramafics were not exposed on the seafloor and did not undergo scouring, which started in the Baimak–Buribai time (Early Devonian) on the eve of the olistostrome formation. The sedimentary rocks of this age contain ultramafic blocks and clastic chromite grains, and serpentinite–sulfide sandstone overlaps the ultramafic bodies.

The Re–Os age of the sulfides from the Dergamysh deposit, the best preserved, is 366 ± 2 Ma (Gannoun et al., 2003). This estimate is comparable with the age of the Zilair Flysch (365 ± 5 Ma), which marks the beginning of the collision (Puchkov, 2000).

Ore formation. The data on the structure of the ore field and the age of the ore mineralization allowed us to correlate the formation of the primary and superimposed ore mineral assemblages with the subduction- and collision-related stages (Fig. 11). The main body of the primary sulfide ore, composed of the minerals belonging to assemblages 1 and 2, was formed at the subduction-related stage. The ore-bearing system comprised (1) the hydrothermal metasomatic massive ore that was formed near the bottom and hosted in serpen-

tinites; (2) the talc–carbonate metasomatic rocks and carbonated serpentinite with stringer–disseminated ore mineralization; (3) the serpentinite–carbonate breccias bearing sulfides (fragments of ore-feeding conduits); and (4) the clastic serpentinite–sulfide ore.

The ore deposition proceeded near the bottom in the course of the hydrothermal metasomatic process. The early pyrite–pyrrhotite massive, the stringer–disseminated pentlandite–pyrite–pyrrhotite, and the chalcopyrite–pyrrhotite ores were deposited in serpentinite and talc–carbonate metasomatic rock. The replacement of ultramafic rocks is recorded in abundant chromite contained in the ore.

The clastic ore, i.e., serpentinite–sulfide gravelstone and sandstone, was formed on the eroded surface of ultramafic rocks as a result as scouring of massive and stringer–disseminated ores. The occurrence of the clastic ore serves as evidence for the exposure and scouring of both the massive sulfide ore and ultramafic rocks on the seafloor. The clastic material contains a great quantity of chromite similar in composition to the chromite from the ultramafic host rocks (Dunaev and Churin, 2003). The primary ore formation was completed by superposition of chalcopyrite I and deposition of the massive and stringer–disseminated chalcopyrite–pyrite–pyrrhotite ore.

The superimposed stringer–disseminated ore mineralization, including arsenides–sulfoarsenides, gold, and tellurides, is referred to the collision stage of the ore field evolution. This looks reasonable by analogy with various polygenetic and multistage deposits in the MUFZ that experienced collision with enrichment in Au and As (Sazonov et al., 2001). The massive sulfide deposits that were not affected by collision do not have such an abundance of veins with As-bearing mineralization, and their accessory sulfoarsenides and arsenides do not contain such diverse admixtures. The fourth mineral assemblage completed the formation of hypogene ore.

COMPARISON OF ANCIENT AND RECENT MASSIVE SULFIDE LODES HOSTED IN ULTRAMAFIC ROCKS

Several active hydrothermal fields associated with ultramafics are known to date: Logachev, 24°30′, Rainbow, Menez Home, Saldanha, Lost City, and Ashadze (Bogdanov, 1997; Bogdanov et al., 1997, 2002, 2004; Beltenev et al., 2003). Furthermore, some other areas of hydrothermal activity are connected with ultramafic rocks to various extents (Melekestseva, 2004). All of them are located in the slowly spreading segments of the Mid-Atlantic Ridge and related to the deep-seated circulation system (Bogdanov et al., 2004).

It is believed that direct counterparts of the currently formed ore hosted in the ultramafic rocks of the present-day mid-ocean ridges have not yet been found among older massive sulfide deposits (Bogdanov et al., 2004). In opinion of F. Barriga (personal communication), such objects may be rare or rarely retained on the seafloor; near-bottom serpentinites, which are prevalent at the slow-spreading ridges, may be obducted only occasionally and hence are not widespread in ophiolites. Foreign researchers consider the Proterozoic copper massive sulfide and Cu–Ni deposits (Outokumpu, Langmuir, Kambalda, etc.) associated to some extent with ultramafic rocks to be allied in origin to the recent sulfides.

In our opinion, the Paleozoic copper massive sulfide deposits hosted in the ultramafic rocks of the MUFZ are more suitable for comparison with recent sulfides because they not only are related to the ultramafic rocks spatially and geochemically but also retained structural and textural features of ore that directly indicate its near-bottom origin and are similar to those in recent ore. These features are the most spectacular at the Dergamysh and Ishkinino deposits (Zaikov et al., 2001; Melekestseva and Zaikov, 2003). The massive colloform and banded ores at the Dergamysh deposit, the serpentinite–sulfide ore clasts (gravelstone and sandstone) with gradational bedding, the psammitic and psephitic fragments with their internal structure truncated by the outer surface, the colloform pyrite–marcasite nodules at the Dergamysh deposit, and the collomorph zonal pyrite–pyrrhotite aggregates at the Ishkinino deposit (Figs. 12a, 12b) serve as examples. Latticed intergrowths of tabular pyrrhotite in the lithic matrix (Fig. 12c) similar to those in chimneys of black smokers at the Rainbow hydrothermal field (Fig. 12d) have been found at the Ivanovka deposit.

Relics of black smokers, known at some massive sulfide deposits of the southern Urals (Maslennikov, 1999; Zaikov et al., 2001), have not yet been found at the deposits located in the MUFZ and hosted in ultramafic rocks. However, it should be kept in mind that the ore deposition at massive sulfide deposits often proceeded below the seafloor.

The occurrence of pyrrhotite as the earliest sulfide is a mineralogical feature of both ancient and recent sulfide bodies hosted in ultramafic rocks. In some areas of the Rainbow field, pyrrhotite amounts to 90% of the bulk sulfides (Vikent'ev et al., 2000). The Co–Ni mineralization of recent ore is represented by millerite, pentlandite, cobalt pentlandite, cobaltite and arsenides of the loellingite–safflorite series, linnaeite, and nickeline (Mozgova et al., 1996; Vikent'ev et al., 2000; Lein et al., 2003; Bortnikov et al., 2004).

Comparison of Co–Ni minerals from recent and ancient ores shows that the ancient ore is richer in these minerals because a long history postdated the initial deposition on the seafloor. The superimposed hydrothermal processes led to the redistribution of cobalt and nickel in ore and to the deposition of sulfoarsenides and arsenides. Under the conditions of recent mineral for-

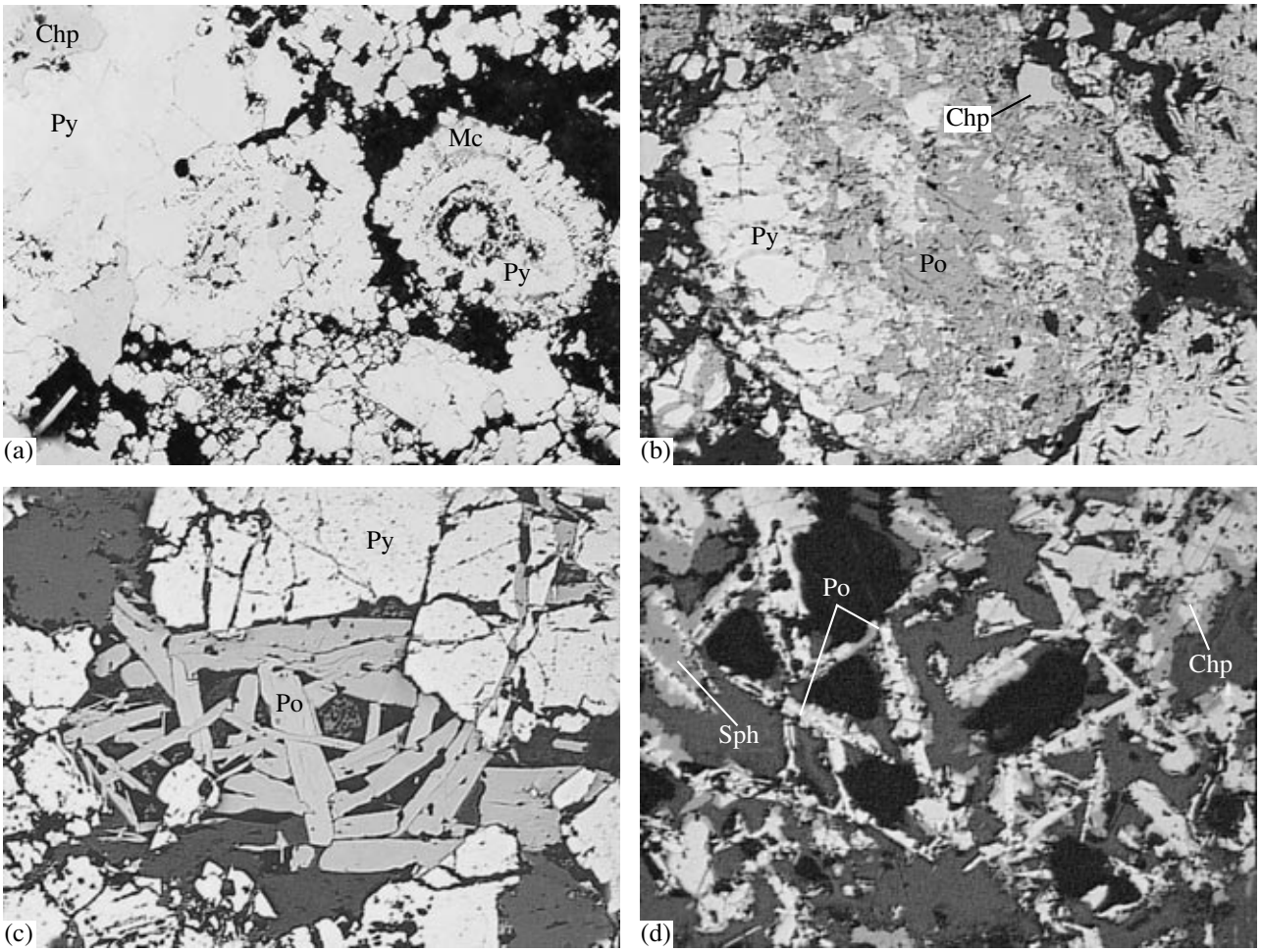

Fig. 12. Structures and textures of ancient and recent ores. (a) Colloform zonal pyrite–marcasite nodules in sulfide sandstone, the Dergamysh deposit, 0.20 mm, sample D1/46.3; (b) colloform zonal pyrite–pyrrhotite aggregates in sulfide sandstone, the Ishkinino deposit, 0.79 mm, sample 332C; (c, d) latticed intergrowths of tabular pyrrhotite: (c) Ivanovka deposit, 0.79 mm, sample Iv2/81.7-2, (d) Rainbow hydrothermal field, 0.38 mm, sample 4402-m1-2/2 from the collection of A.Yu. Lein; black in microphotographs, gangue minerals.

mation, the system remains unstable, and many phases in recent ore, including the Ni–Co minerals, are metastable and nonstoichiometric and may be rather called protominerals. However, the ability to produce such ore mineralization draws together the ancient and recent ores hosted in ultramafic rocks.

The physicochemical parameters of ore formation at the Ishkinino deposit estimated with thermobarogeochemical methods are close to those at the Rainbow field (salinity, composition, and temperature of hydrothermal solutions). The salinity of hydrothermal solutions that created the Ishkinino deposit reached 7.1 wt %, whereas at the Rainbow field it reaches 7.7 wt %; NaCl with an insignificant admixture of KCl prevails at both localities. The temperature of hydrothermal solutions at the Ishkinino deposit is estimated at 150–200°C, and at the Rainbow field, at 177–198°C (Yuminov et al., 2002).

The most important difference in the objects under comparison is related to the geodynamic conditions of the ore formation. Recent sulfide deposition on ultramafic rocks was discovered in slowly spreading segments of the Mid-Atlantic Ridge, where serpentinization takes place. In contrast, serpentinites at the Ishkinino deposit are suprasubduction ultramafics with specific chromites. In this regard, it was suggested that sulfides might be found in the accretionary wedges of the active island arcs containing sheets of ultramafic rocks.

CONCLUSIONS

The geological setting and formation conditions of massive sulfide bodies at the Ishkinino deposit hosted in ultramafic rocks of the Main Ural Fault Zone have been studied. In terms of paleotectonics, the ore field is related to an Early Devonian accretionary prism made up of ophiolitic and island-arc tectonic sheets. In the

present-day structure, the ore field is an antiform that arose at the collision stage.

The structural–textural and mineralogical–geochemical features of Co–Cu massive sulfide ore hosted in conglomerate-like and massive serpentinites and talc–carbonate metasomatic rocks are recognized. The primary ore formed at the island-arc stage of the evolution of foldbelt is opposed to the ore transformed at the collision stage. The examination of samples with ore microscopy resulted in revealing of cobalt diarsenides, as well as Fe and Ni diarsenides, including loellingite, safflorite, rammelsbergite, and krutovite.

Ancient and recent sulfides associated with ultramafic rocks were compared and their similar and distinct features were demonstrated.

ACKNOWLEDGMENTS

We thank V.V. Maslennikov, E.V. Belogub, K.A. Novoselov, S.G. Tesalina, V.A. Popov, L.Ya. Kabanova, A.M. Yuminov, G.G. Korablev, A.Yu. Dunaev, R.R. Shavaleev, M.M. Boldyreva, V.A. Simonov, B. Buschmann and P. Jonas (Freiberg, Germany), and P. Nimis (Padua, Italy) for their critical comments, helpful advice, and consultations in the course of investigations. We are also grateful to V.A. Kotlyarov, E.I. Churin, K. Becker (Freiberg), J. Spratt (London), N.S. Rudashevsky, and Yu.L. Kretser for analytical studies.

The work was supported by program no. 14 of the Presidium of the Russian Academy of Sciences ("The World Ocean: Geology, Geodynamics, Physics, and Biology,") by the project "Comparative Analysis of the Mineralogy, Geochemistry, and Biochemistry of Sulfide Ores of the Present-Day and Paleozoic Oceans," and by the Russian Foundation for Basic Research (project no. 04-05-96014-r2004Ural).

REFERENCES

1. V. Beltenev, A. Nescheretov, V. Shilov, et al., "New Discoveries at 12°58′ N and 44°52′ W MAR: Initial Results from the Professor Logatchev-22 Cruise," InterRidge News **12** (1), 13–15 (2003).
2. Yu. A. Bogdanov, N. S. Bortnikov, I. V. Vikent'ev, et al., "A New Type of Modern Mineral-Forming System: Black Smokers of the Hydrothermal Field at 14°15′ N Latitude, Mid-Atlantic Ridge," Geol. Rudn. Mestorozhd. **39** (1), 68–90 (1997) [Geol. Ore Deposits **39** (1), 58–78 (1997)].
3. Yu. A. Bogdanov, N. S. Bortnikov, I. V. Vikent'ev, et al., "Mineralogical–Geochemical Peculiarites of Hydrothermal Sulfide Ores and Fluids in the Rainbow Field Associated with Serpentinites, Mid-Atlantic Ridge (36°47′ N)," Geol. Rudn. Mestorozhd. **44** (6), 513–545 (2002) [Geol. Ore Deposits **44** (6), 444–473 (2002)].
4. Yu. A. Bogdanov, A. Yu. Lein, N. S. Bortnikov, and A. M. Sagalevich, "Hydrothermal Inclusions from Serpentinite Massifs on Oceanic Floor," Izv. Sektsii Nauk Zemle Ross. Akad. Estestv. Nauk, No. 12, 63–90 (2004).
5. B. S. Borishanskaya, R. A. Vinogradova, and G. A. Krutov, *Cobalt and Nickel Minerals* (Moscow State Univ., Moscow, 1981) [in Russian].
6. N. S. Bortnikov, V. A. Simonov, and Yu. A. Bogdanov, "Fluid Inclusions in Minerals from Modern Sulfide Mounds: Physicochemical Conditions of Mineral Formation and Fluid Evolution," Geol. Rudn. Mestorozhd. **46** (1), 74–87 (2004) [Geol. Ore Deposits **46** (1), 64–75 (2004)].
7. E. S. Buchkovsky, "Sulfide Mineralization Related to Ultramafic Intrusions on the Western Limb of the Magnitogorsk Megasynclinorium in the Southern Urals," in *Geology, Mineralogy, and Geochemistry of Massive Sulfide Deposits in the Southern Urals* (Inst. Geol., Bashkir. Branch, Acad. Sci. USSR, Ufa, 1970), pp. 114–125 [in Russian].
8. H. J. B. Dick and T. Bullen, "Chromian Spinel As a Petrogenetic Indicator in Abyssal and Alpine-type Peridotites and Spatially Associated Lavas," Contrib. Min. Petrol. **86**, 54–76 (1984).
9. A. Yu. Dunaev and E. I. Churin, "Accessory Cr-Spinel from Ultramafic Rocks of Ishkinino Cobalt–Copper Massive Sulfide Deposit (Southern Urals)," in *Metallogeny of Ancient and Modern Oceans, 2003. Origin and Exploration of Ore Deposits in Island-Arc Systems* (Inst. Mineral., Miass, 2003), pp. 226–231 [in Russian].
10. A. Gannoun, S. Tessalina, B. Bourdon, et al., "Re–Os Isotopic Constraints on the Genesis and Evolution of the Dergamish and Ivanovka Cu (Co, Au) Massive Sulphide Deposits, South Urals, Russia," Chem. Geol. **190**, 1–15 (2003).
11. P. Jonas, *Tectonostratigraphy of Oceanic Crustal Terrains Hosting Serpentinite-Associated Massive Sulfide Deposits in the Main Uralian Fault Zone (South Urals)* (PhD Thesis, Freiberg, 2003).
12. V. Kamenetsky, A. Crawford, and S. Meffre "Factors Controlling Chemistry of Magmatic Spinel: An Empirical Study of Associated Olivine, Cr-Spinel and Melt Inclusions from Primitive Rocks," J. Petrol. **42**, 655–671 (2001).
13. E. S. Kontar and L. E. Libarova, *Metallogeny of Copper, Zinc, and Lead in the Urals* (Uralgeolkom, Yekaterinburg, 1997) [in Russian].
14. I. Kostov and J. Minčeva-Stefanova, *Sulfide Minerals: Crystal Chemistry, Parageneses, and Systematics* (Bulgarian Acad. Sci., Sofia, 1981; Mir, Moscow, 1984).
15. A. Yu. Lein, G. A. Cherkashev, A. A. Ul'yanov, et al., "Mineralogy and Geochemistry of Sulfide Ores from the Logachev-2 and Rainbow Fields: Similar and Distinctive Features," Geokhimiya **41** (3), 304–328 (2003) [Geochem. Int. **41** (3), 271–294 (2003)].
16. V. V. Maslennikov, *Sedimentogenesis, Halmyrolysis, and Ecology of Paleohydrothermal Massive Sulfide Ore Fields* (Geotur, Miass, 1999) [in Russian].
17. I. Yu. Melekestseva, "Register of Hydrothermal Systems with Ore Mineralization in the World Ocean," in *Metallogeny in Ancient and Modern Oceans, 2004. Achievements on the Turn of the Century* (Inst. Mineral., Miass, 2004), Vol. II, pp. 232–252 [in Russian].
18. I. Yu. Melekestseva and V. V. Zaikov, *Ores of the Ishkinino Cobalt–Copper Massive Sulfide Deposit (Southern Urals)* (Inst. Mineral., Miass, 2003) [in Russian].

19. *Metallogeny of Island-Arc Geodynamic Settings*, Ed. by N. V. Mezhelovsky (Geokart, Moscow, 1999) [in Russian].

20. N. N. Mozgova, S. G. Krasnov, B. N. Batuev, et al., "The First Report of Cobalt Pentlandite from a Mid-Atlantic Ridge Hydrothermal Deposit," Can. Mineral. **34** (1), 23–28 (1996).

21. V. N. Puchkov, *Paleogeodynamics of the Southern and Central Urals* (Dauriya, Ufa, 2000) [in Russian].

22. V. N. Sazonov, V. N. Ogorodnikov, V. A. Koroteev, and Yu. A. Polenov, *Gold Deposits in the Urals* (UGGGA, Yekaterinburg, 2001) [in Russian].

23. I. B. Seravkin, S. E. Znamensky, and A. M. Kosarev, "The Main Ural Fault in the Southern Urals: the Structure and Main Evolution Phases," Geotektonika, **37** (3), 42–64 (2003) [Geotectonics **37** (3), 210–231 (2003)].

24. V. A. Simonov, V. V. Zaikov, B. Bushmann, and S. V. Kovyazin, "Formation Conditions of Basaltoids at the Ishkinino Massive Sulfide Deposit (Southern Urals)," in *Metallogeny of Ancient and Modern Oceans, 2000. Discovery, Appraisal, and Development of Mineral Deposits* (Inst. Mineral., Miass, 2000), pp. 174–181 [in Russian].

25. V. A. Simonov, V. V. Zaikov, and Yu. P. Kolmogorov, "Geochemistry of Basaltic Rocks from Ophiolite and Suture Zones in Southern Urals," in *Metallogeny of Ancient and Modern Oceans, 2002. Origin and Exploration of Mineral Deposits in Ophiolite Zones* (Inst. Mineral., Miass, 2002), pp. 17–26 [in Russian].

26. *Stratigraphy and Correlation of Middle Paleozoic Volcanic Complexes in the Main Copper Massive Sulfide Districts of the Southern Urals* (Ufa Sci. Center, Russ. Acad. Sci., Ufa, 1993) [in Russian].

27. S. G. Tesalina, P. Nimis, T. Augé, and V. V. Zaykov, "Origin of Chromite in Mafic-Ultramafic-Hosted Hydrothermal Massive Sulfides from the Main Uralian Fault, South Urals, Russia," Lithos **70**, 39–59 (2003).

28. A. S. Varlakov, *Petrography, Petrochemistry, and Geochemistry of Ultramafics in the Orenburg Urals* (Nauka, Moscow, 1978) [in Russian].

29. I. V. Vikent'ev, N. S. Bortnikov, Yu. A. Bogdanov, et al., "Mineralogy of Hydrothermal Deposits of the Rainbow Field in the Azores Region (Atlantic Ocean)," in *Metallogeny of Ancient and Modern Oceans, 2002. Discovery, Appraisal, and Development of Mineral Deposits* (Inst. Mineral., Miass, 2000), pp. 103–110 [in Russian].

30. A. M. Yuminov, V. A. Simonov, and V. V. Zaikov, "Physicochemical Parameters of Hydrothermal Processes at the Ishkinino Massive Sulfide Deposit (Southern Urals)," in *Ural Mineral. Sbornik*, No. 12, 98–110 (2002).

31. V. V. Zaikov, V. V. Maslennikov, E. V. Zaikova, and R. Herrington, *Typification and Ore Facies of the Massive Sulfide Deposits of the Ural Paleocean* (Inst. Mineral., Miass, 2001) [in Russian].

32. A. A. Zakharov and A. A. Zakharova, "Genesis of Sulfide Ore at the Copper–Cobalt Deposits of the Ivanovka Group in the Southern Urals," in *Proceedings of II Ural Conference of Young Geologists and Geophysicists on the Geology and Mineral Resources of the Urals* (Sverdlovsk, 1969), Part II, pp. 53–55 [in Russian].